52| Dispense 250 µl of 240 OD per ml extract and 1 µl of 20 mg ml^{-1} creatine kinase into each fresh microtubes on ice.

53| Resuspend the mRNA solutions, which contain white insoluble material, and transfer 250 µl of each suspension into each microtube containing the extract and creatine kinase. Mix the samples gently by pipetting, avoiding bubbles.

54| Dispense 5.5 ml of 1× BSS in each well of a flat-bottomed six-well plate.

55| Take each of the mRNA/extract mixtures into a micropipette tip so that no air is at the end of the tip. Insert the tip at the bottom of a microtiter well containing 1× BSS carefully by holding the mixture within the tip and then carefully pump out the mixture under the buffer without mixing, avoiding bubbles, so that the mRNA/extract mixture and the buffer form a bilayer. Do not mix the samples. Do not shake the plate.
▲ **CRITICAL STEP** Do not mix the samples. It is very important at the start of the reaction that the starting reaction mixture forms a distinct layer that forms a clear boundary with the upper BSS liquid.

56| Seal the plate to avoid evaporation. Be careful not to shake the plate too much.

57| Leave the plate in the air incubator at 15 °C for 20 h.

58| After the incubation, mix the samples for further analyses.

59| To check the products, load 3 µl of the samples on a standard SDS gel.
? TROUBLESHOOTING

● **TIMING**
Steps 1–8, preparation of unwashed embryo particles: 2–3 d per 5 g embryo particles from 5 to 6 kg seeds
Steps 9–27, preparation of the extract: 1 d
Steps 28–37, template DNA preparation for small-scale parallel protein synthesis: 1 day
Steps 38 and 39, mRNA preparation for small-scale parallel protein synthesis: 5–7 h
Steps 40–47, small-scale parallel protein synthesis: 1 h + an overnight reaction (20 h) + 3 h
Step 48–50, transcription of a pEU plasmid harboring a target ORF sequence: 5–7 h excepting Step 48
Steps 51–59, large-scale protein synthesis: 1 h + an overnight reaction (20 h) + 3 h

? TROUBLESHOOTING
Troubleshooting advice can be found in **Table 2**. In our experience, most of the troubles come from a problem during the construction of the DNA molecules that are used for PCR and/or transcription.

TABLE 2 | Troubleshooting table.

Step	Problem	Possible reason	Solution
23	Low absorbance	Grinding was not sufficient	This could be foreseen by the color of the supernatant in Step 19
26	Absorbance lower than 240	Insufficient condensation in Step 24	Concentrate the sample again, or leave it as it is
29	No band	Bad template	Check the template cDNA. The plasmid should have the pUC origin and the cDNA sequence
		The specific primer does not hybridize well	Lower the annealing temperature of the PCR program. Extend the target region of the primer
		Primer-dimer involving the specific primer	Extend the target region of the primer
	Nonspecific bands	Hybridization of AODA2306 within the ORF	Try proceeding to Steps 30–37. If the result is still bad, try another primer that hybridizes near the replication origin. For screening purposes, judge if one wishes to stick to this sample
37	No band	Loss of the pellet in the Step 33 or 35	Restart from Step 30
	Nonspecific bands	Nonspecific hybridization within the ORF	Try translation if the main band is correct. For screening purposes, judge if one wishes to stick to this sample

(continued)

TABLE 2 | Troubleshooting table (continued).

Step	Problem	Possible reason	Solution
39	No band	dNTP instead of NTP added to the reaction	Try again being careful not to confuse NTP with dNTP
	Ladder in the high mobility region	Contamination by Rnases	Extract the template DNA with phenol/chloroform
	Unexpected low mobility extra bands	Efficient transcription	This usually causes no problem in translation
	Very bright bands	Sample is not denatured and is complexed with Spermidine	Denature the sample in a formamide loading dye, which may be the one used for denaturing gels, before applying to the gel
47 or 59	No product	Bad mRNA	Check the mRNA and template DNA again
	No or very faint band	Inefficient translation	Try the small-scale translation again with ^{14}C-labeled leucine added to the reaction and BSS and detect the product by autoradiography or by counting the radioactivity in the acid-insoluble fraction of the reaction mixture
		Alternative translation initiation (out of frame)	Eliminate Gs from between the E01 enhancer sequence and the initiation codon
	Doublet band	Alternative translation initiation (in frame)	Eliminate Gs from between the E01 enhancer sequence and the initiation codon
50	Smear or ladder in the high-mobility region	Contamination by RNase	Further purify the plasmid template as in Step 47
	No band	dNTP instead of NTP added to the reaction	Try again being careful not to confuse NTP with dNTP
		Bad plasmid	Check the plasmid DNA
59	No band	Bad plasmid	Check the plasmid DNA
	Unexpected bands in the low-mobility region	Post-translational modification	Post-translational modification may occur for some proteins We have no unified methodology

ANTICIPATED RESULTS

We show here a typical result of small-scale bilayer mode synthesis of fluorescent proteins (**Fig. 5b**). An SDS gel showing a typical result of synthesis of dihydrofolate reductase (DHFR) is in **Figure 6**. It is difficult to show an averaged amount of produced protein per 1-ml reaction because we do not have a reliable statistic data with the protocol shown here and because the productivity per reaction volume including BSS can vary with the relative volume of BSS to the reaction mixture. However, the average yield per

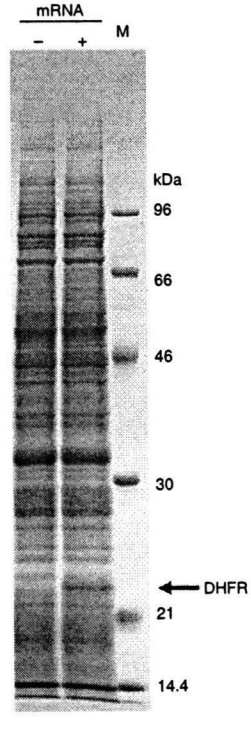

Figure 6 | A typical result of the small-scale bilayer synthesis of DHFR. DHFR was synthesized by the bilayer method using the CFS extract (CFS-TRI-1240), and a 3-μl aliquot of the mixed sample was separated on an SDS gel stained with CBB (Step 47). The left lane (mRNA+), a control reaction product with no mRNA added; the center lane (mRNA–), the product with the DHFR mRNA; and the right lane (M), marker proteins with molecular masses indicated on the right. The amount of DHFR synthesized was 80 ng μl^{-1} (1.8 mg per 1-ml extract). In the parallel protein synthesis experiments, the 'mRNA–' reaction can usually be omitted because different samples can serve as the markers indicating the positions of the bands of the wheat embryo proteins. Modified from a figure kindly provided by R. Morishita, CellFree Sciences.

1-ml extract may be around 0.3 mg both in the small- and large-scale bilayer method. In fact, the average amount per a 150-µl reaction containing 12 µl of the extract for the 13,000 different human ORFs was 4.2 µg, which means 0.35 mg per 1-ml extract[7].

ACKNOWLEDGMENTS This work was supported in part by the Special Coordination Funds for Promoting Science and Technology (Y.E.) and in part by a Grant-in-Aid for Scientific Research on the Priority Areas (No. 20034040 to K.T.) by the Ministry of Education, Culture, Sports, Science and Technology, Japan. We are grateful to Dr. R. Morishita and Mr. Y. Tanaka of CFS for providing pictures and for checking the paper.

AUTHOR CONTRIBUTIONS K.T. collected information and wrote the paper; T.S. prepared the data and pictures; and Y.E. supervised the study.

Published online at http://www.natureprotocols.com/.
Reprints and permissions information is available online at http://npg.nature.com/reprintsandpermissions/.

1. Spirin, A.S., Baranov, V.I., Ryabova, L.A., Ovodov, S.Y. & Alakhov, Y.B. A continuous cell-free translation system capable of producing polypeptides in high yield. *Science* **242**, 1162–1164 (1988).
2. Madin, K., Sawasaki, T., Ogasawara, T. & Endo, Y. A highly efficient and robust cell-free protein synthesis system prepared from wheat embryos: plants apparently contain a suicide system directed at ribosomes. *Proc. Natl. Acad. Sci. USA* **97**, 559–564 (2000).
3. Sawasaki, T., Ogasawara, T., Morishita, R. & Endo, Y. A cell-free protein synthesis system for high-throughput proteomics. *Proc. Natl. Acad. Sci. USA* **99**, 14652–14657 (2002).
4. Sawasaki, T. *et al.* A bilayer cell-free protein synthesis system for high-throughput screening of gene products. *FEBS Lett.* **514**, 102–105 (2002).
5. Endo, Y. & Sawasaki, T. Cell-free expression systems for eukaryotic protein production. *Curr. Opin. Biotechnol.* **17**, 373–380 (2006).
6. Takai, K., Sawasaki, T. & Endo, Y. Development of key technologies for high-throughput cell-free protein production with the extract from wheat embryos. *Adv. Protein Chem. Struct. Biol.* **75**, 53–84 (2008).
7. Goshima, N. *et al.* Human protein factory for converting the transcriptome into an *in vitro*-expressed proteome. *Nat. Methods* **5**, 1011–1017 (2008).
8. Tsuboi, T. *et al.* Wheat germ cell-free system-based production of malaria proteins for discovery of novel vaccine candidates. *Infect. Immun.* **76**, 1702–1708 (2008).
9. Sawasaki, T. *et al.* The wheat germ cell-free expression system: methods for high-throughput materialization of genetic information. *Methods Mol. Biol.* **310**, 131–144 (2005).
10. Sawasaki, T. & Endo, Y. Chapter 6. Protein expression in the wheat-germ cell-free system. In *Expression Systems* (eds. Dyson, M.R. & Durocher, Y.) 87–108 (Scion Publishing Ltd., Oxfordshire, Oxford, UK, 2007).
11. Endo, Y., Dohi, N. & Nakagawa, M. Germ extract for cell-free protein synthesis and process for producing the same. International Patent WO/2003/064671 filed 31 January 2003.
12. Kamura, N., Sawasaki, T., Kasahara, Y., Takai, K. & Endo, Y. Selection of 5′-untranslated sequences that enhance initiation of translation in a cell-free protein synthesis system from wheat embryos. *Bioorg. Med. Chem. Lett.* **15**, 5402–5406 (2005).
13. Masaoka, T., Nishi, M., Ryo, A., Endo, Y. & Sawasaki, T. The wheat germ cell-free based screening of protein substrates of calcium/calmodulin-dependent protein kinase II delta. *FEBS Lett.* **582**, 1795–1801 (2008).
14. Makino, S., Sawasaki, T., Tozawa, Y., Endo, Y. & Takai, K. Covalent circularization of exogenous RNA during incubation with a wheat embryo cell extract. *Biochem. Biophys. Res. Commun.* **347**, 1080–1087 (2006).
15. Hirano, N., Sawasaki, T., Tozawa, Y., Endo, Y. & Takai, K. Tolerance for random recombination of domains in prokaryotic and eukaryotic translation systems: limited interdomain misfolding in a eukaryotic translation system. *Proteins* **64**, 343–354 (2006).
16. Nureki, O. *et al.* Deep knot structure for construction of active site and cofactor binding site of tRNA modification enzyme. *Structure* **12**, 593–602 (2004).
17. Ikeda, K. *et al.* Immobilization of diverse foreign proteins in viral polyhedra and potential application for protein microarrays. *Proteomics* **6**, 54–66 (2006).
18. Matsumoto, K. *et al.* Production of yeast tRNA (m^7G46) methyltransferase (Trm8-Trm82 complex) in a wheat germ cell-free translation system. *J. Biotechnol.* **133**, 453–460 (2008).
19. Kanno, T., Kasai, K., Ikejiri-Kanno, Y., Wakasa, K. & Tozawa, Y. *In vitro* reconstitution of rice anthranilate synthase: distinct functional properties of the alpha subunits OASA1 and OASA2. *Plant Mol. Biol.* **54**, 11–22 (2004).
20. Takahashi, H., Nozawa, A., Seki, M., Shinozaki, K., Endo, Y. & Sawasaki, T. A simple and high-sensitivity method for analysis of ubiquitination and polyubiquitination based on wheat cell-free protein synthesis. *BMC Plant Biol.* **9**, 39 (2009).
21. Kanno, T. *et al.* Sequence specificity and efficiency of protein N-terminal methionine elimination in wheat-embryo cell-free system. *Protein Expr. Purif.* **52**, 59–65 (2007).
22. Kobayashi, T., Kodani, Y., Nozawa, A., Endo, Y. & Sawasaki, T. DNA-binding profiling of human hormone nuclear receptors via fluorescence correlation spectroscopy in a cell-free system. *FEBS Lett.* **582**, 2737–2744 (2008).
23. Sawasaki, T. *et al.* Arabidopsis HY5 protein functions as a DNA-binding tag for purification and functional immobilization of proteins on agarose/DNA microplate. *FEBS Lett.* **582**, 221–228 (2008).
24. Kanno, T. *et al.* Structure-based *in vitro* engineering of the anthranilate synthase, a metabolic key enzyme in the plant tryptophan pathway. *Plant Physiol.* **138**, 2260–2268 (2005).
25. Morita, E.H., Sawasaki, T., Tanaka, R., Endo, Y. & Kohno, T. A wheat germ cell-free system is a novel way to screen protein folding and function. *Protein Sci.* **12**, 1216–1221 (2003).
26. Vinarov, D.A. *et al.* Cell-free protein production and labeling protocol for NMR-based structural proteomics. *Nat. Methods* **1**, 149–153 (2004).
27. Vinarov, D.A., Loushin Newman, C.L. & Markley, J.L. Wheat germ cell-free platform for eukaryotic protein production. *FEBS J.* **273**, 4160–4169 (2006).
28. Morita, E.H. *et al.* A novel way of amino acid-specific assignment in ^1H-^{15}N HSQC spectra with a wheat germ cell-free protein synthesis system. *J. Biomol. NMR* **30**, 37–45 (2004).
29. Kohno, T. Production of proteins for NMR studies using the wheat germ cell-free system. *Methods Mol. Biol.* **310**, 169–185 (2005).
30. Kohno, T. & Endo, Y. Production of protein for nuclear magnetic resonance study using the wheat germ cell-free system. *Methods Mol. Biol.* **375**, 257–272 (2007).
31. Kainosho, M. *et al.* Optimal isotope labelling for NMR protein structure determinations. *Nature* **440**, 52–57 (2006).
32. Miyazono, K. *et al.* Novel protein fold discovered in the PabI family of restriction enzymes. *Nucleic Acids Res.* **35**, 1908–1918 (2007).
33. Abe, M. *et al.* Detection of structural changes in a cofactor binding protein by using a wheat germ cell-free protein synthesis system coupled with unnatural amino acid probing. *Proteins* **67**, 643–652 (2007).
34. Kawasaki, T., Gouda, M.D., Sawasaki, T., Takai, K. & Endo, Y. Efficient synthesis of a disulfide-containing protein through a batch cell-free system from wheat germ. *Eur. J. Biochem.* **270**, 4780–4786 (2003).
35. Nozawa, A. *et al.* A cell-free translation and proteoliposome reconstitution system for functional analysis of plant solute transporters. *Plant Cell Physiol.* **48**, 1815–1820 (2007).
36. Goren, M.A. & Fox, B.G. Wheat germ cell-free translation, purification, and assembly of a functional human stearoyl-CoA desaturase complex. *Protein Expr. Purif.* **62**, 171–178 (2008).
37. Kaiser, L., Graveland-Bikker, J., Steuerwald, D., Vanberghem, M., Herlihy, K. & Zhang, S. Efficient cell-free production of olfactory receptors: detergent optimization, structure, and ligand binding analyses. *Proc. Natl. Acad. Sci. USA* **105**, 15726–15731 (2008).

THE JOURNAL OF BIOLOGICAL CHEMISTRY VOL. 284, NO. 42, pp. 28642–28649, October 16, 2009

Paraquat Toxicity Induced by Voltage-dependent Anion Channel 1 Acts as an NADH-dependent Oxidoreductase*[S]

Received for publication, June 12, 2009, and in revised form, August 7, 2009 Published, JBC Papers in Press, August 28, 2009, DOI 10.1074/jbc.M109.033431

Hiroki Shimada[‡1], Kei-Ichi Hirai[§], Eriko Simamura[‡], Toshihisa Hatta[‡], Hiroki Iwakiri[¶], Keiji Mizuki[¶], Taizo Hatta[¶], Tatsuya Sawasaki[‖], Satoko Matsunaga[‖], Yaeta Endo[‖**], and Shigeomi Shimizu[‡‡]**

*From [‡]Molecular and Cell Structural Science, Kanazawa Medical University, Uchinada, Ishikawa 920-0293, the [§]Niwa Institute for Immunology, Tosashimizu, Kochi 787-0306, the [¶]Department of Nanoscience, Sojo University, Ikeda, Kumamoto 860-0082, the [‖]Cell-free Science and Technology Research Center and the Venture Business Laboratory, Ehime University, Matsuyama, Ehime 790-8577, the **RIKEN Genomic Sciences Center, Tsurumi, Yokohama 230-0045, and the [‡‡]Department of Pathological Cell Biology, Medical Research Institute, Tokyo Medical and Dental University, Yushima, Bunkyo, Tokyo 113-8510, Japan*

Paraquat (PQ), a herbicide used worldwide, causes fatal injury to organs upon high dose ingestion. Treatments for PQ poisoning are unreliable, and numerous deaths have been attributed inappropriate usage of the agent. It is generally speculated that a microsomal drug-metabolizing enzyme system is responsible for PQ toxicity. However, recent studies have demonstrated cytotoxicity via mitochondria, and therefore, the cytotoxic mechanism remains controversial. Here, we demonstrated that mitochondrial NADH-dependent PQ reductase containing a voltage-dependent anion channel 1 (VDAC1) is responsible for PQ cytotoxicity. When mitochondria were incubated with NADH and PQ, superoxide anion ($O_2^{\cdot-}$) was produced, and the mitochondria ruptured. Outer membrane extract oxidized NADH in a PQ dose-dependent manner, and oxidation was suppressed by VDAC inhibitors. Zymographic analysis revealed the presence of VDAC1 protein in the oxidoreductase, and the direct binding of PQ to VDAC1 was demonstrated using biotinylated PQ. VDAC1-overexpressing cells showed increased $O_2^{\cdot-}$ production and cytotoxicity, both of which were suppressed in VDAC1 knockdown cells. These results indicated that a VDAC1-containing mitochondrial system is involved in PQ poisoning. These insights into the mechanism of PQ poisoning not only demonstrated novel physiological functions of VDAC protein, but they may facilitate the development of new therapeutic approaches.

Paraquat (PQ^2; methyl viologen, 1,1′-dimethyl-4,4′-bipyridinium dichloride) is an effective herbicide used in more than 120 countries (1). Although it is classified as a low hazard compound, PQ is hazardous when used improperly and has been found responsible for thousands of deaths worldwide because of intentional overdose and high levels of occupational and accidental exposure especially in developing countries (1). Direct exposure to PQ causes severe irritation to the eyes and skin, and ingestion of concentrated products may result in fatal injury to lungs because of edema, hemorrhage, and subsequent fibrosis as well as damage to other organs (2). Additionally, PQ has emerged as a risk factor for Parkinson disease (3). The acute toxicity of PQ in mammals is mediated by reactive oxygen species (ROS) produced by a cyclic oxidation-reduction reaction (4). It is generally speculated that NADPH-cytochrome P450 reductase in microsomal drug-metabolizing enzyme systems is responsible for the production of ROS (5). However, we previously observed that the initial ultrastructural alterations associated with PQ exposure occurred only in mitochondria and not in the endoplasmic reticulum in pulmonary cells *in vivo* (6) and *in vitro* (7). In addition, several reports have suggested the cytotoxicity of PQ via mitochondrial dysfunction (8–10). Despite the development of a number of treatments for PQ poisoning, the efficacy and reliability of currently available treatments have remained limited because of an insufficient understanding of PQ cytotoxicity (2).

We recently discovered that active NADH-dependent oxidoreductase located on the mitochondrial outer membrane reduced PQ to a radical form that spontaneously formed superoxide anion ($O_2^{\cdot-}$) and destroyed mitochondria (11–13). Furthermore, we demonstrated that 1) PQ was initially metabolized to monopyridone in the cytosol and subsequently hydroxylated by the microsomes and 2) the induction of drug-metabolizing enzymes and the administration of a ROS scavenger reduced PQ toxicity in mice (11, 14). These results indicate that the mitochondrial system, not the microsomal system, is responsible for PQ toxicity. We verified that enzymes in the electron transport chain and NADH-cytochrome b_5 reductase, an NADH-dependent oxidoreductase in the outer membrane, were not involved in this reaction (11, 12). A voltage-dependent anion channel (VDAC), an abundant pore-forming protein in the outer membrane, exerts numerous physiological functions as a channel; it regulates both the metabolite flux of mitochondria and transmembrane potential, and plays a role in apoptosis. Recently, it was reported that NADH regulates VDAC func-

* This work was supported by Grants-in-aid for Scientific Research 15591664, 17591899, 19390291, and 21791045 from the Japan Society for the Promotion of Science, Grants for Promoted Research S2003-12, S2004-12, C2007-4, S2007-9, C2008-1, S2008-10, C2009-3, and S2009-10 from Kanazawa Medical University, Grant for Project Research H2009-14 from High-Tech Research Center of Kanazawa Medical University, and in part by The Ministry of Education, Culture, Sports, Science, and Technology, Japan Grant S0801085.

[S] The on-line version of this article (available at http://www.jbc.org) contains supplemental schemes.

[1] To whom correspondence should be addressed. Fax: 81-76-218-8189; E-mail: simada-h@kanazawa-med.ac.jp.

[2] The abbreviations used are: PQ, paraquat; BQ, benzoquinone; DCF, 2′,7′-dichlorofluorescein; DCFH, DCF-diacetate; DIDS, 4,4′-diisothiocyanatostilbene-2,29-disulfic acid; IC_{50}, 50% growth inhibition toxicity; mAb, monoclonal antibody; PTP, permeability transition pore; TBS, Tris-buffered saline; VDAC, voltage-dependent anion channel; ROS, reactive oxygen species; SOD, superoxide dismutase; siRNA, small Interfering RNA.

tion (15), and an isoform of VDAC localized in the plasma membrane possesses NADH-ferricyanide reductase activity (16). Therefore, we attempted to determine whether or not NADH-PQ oxidoreductase on mitochondria is responsible for PQ cytotoxicity and if VDAC participates in this activity.

EXPERIMENTAL PROCEDURES

Cell Line

HeLa cells were provided by RIKEN Cell Bank (Tsukuba, Japan). Cells were cultured in Dulbecco's modified Eagle's medium (Sigma-Aldrich) supplemented with 10% fetal bovine serum at 37 °C in a humidified CO_2 incubator.

Intracellular ROS Production

Mitochondrial superoxide production in HeLa cells was detected using MitoSOX® (Molecular Probes Inc., Eugene, OR), a red fluorescent mitochondrial superoxide indicator, according to the given protocol. Cells were pretreated with 1 mM PQ; Sigma-Aldrich) for 50 min at 37 °C and incubated with 5 μM MitoSOX for 10 min in the dark. The medium was exchanged for fresh medium, and the cells were observed by a fluorescence microscope (Olympus IX70, Olympus Corp., Tokyo, Japan). The effects of benzoquinone (BQ; 0.2 mM, Sigma-Aldrich) were evaluated after 10 min of incubation in BQ-added medium. Intracellular H_2O_2 production in HeLa cells by PQ was detected using 2′,7′-dichlorofluorescein-diacetate (DCFH; Molecular Probes) (17, 18). Briefly, cells were pretreated with 1 mM PQ for 1 h at 37 °C, and then the cells were incubated with 5 μM DCFH for 20 min in the dark. Afterward, the medium was exchanged for fresh medium; fluorescence images that appeared after the formation of 2′,7′-dichlorofluorescein (DCF) were observed by fluorescence microscopy.

Preparation of Mitochondria

Mitochondria were isolated from the livers of male Wistar rats or from HeLa cells by differential centrifugation (11, 12). Mitochondria were suspended in 0.25 M sucrose solution containing 0.05 M Tris-HCl, 20 mM KCl, 2.0 mM $MgCl_2$, and 1.0 mM Na_2HPO_4 (pH 7.4). The mitochondria were starved for 20 min at 37 °C to consume endogenous substrates before use. The Kanazawa Medical University Animal Care and Use Committee approved all studies. All animals were cared for and treated in accordance with the Committee guidelines.

PQ-dependent Hydrogen Peroxide (H_2O_2) Production on Mitochondria

Mitochondria were attached onto a glass-based culture dishes coated with Cell-Tak® (BD Biosciences) (19). The dishes were incubated with 10 mM PQ and 2 mM NADH (Oriental Yeast Co., Ltd., Tokyo, Japan) in the sucrose solution containing 5 μM DCFH, 5 μM rotenone (Sigma-Aldrich), and 1 μM *p*-hydroxymercuribenzoate (Sigma-Aldrich) at 37 °C. Fluorescence images were captured by a digital CCD camera (Pixera Penguin 150 CL, Pixera Corp., Los Gatos, CA) attached to a microscope and were analyzed by Lumina Vision bio-imaging analysis system (Mitani Corp., Fukui, Japan). The fluorescence intensity per 1000 mitochondria was calculated, and the mean value of three areas from each sample was compared. BQ (0.3 mM), anti-VDAC1 monoclonal antibody (mAb; anti-porin 31 HL mAb, 9 μg/ml; Calbiochem), and 4,4′-diisothiocyanatostilbene-2,29-disulfic acid (DIDS; 100 μM, Sigma-Aldrich) were evaluated by addition to the reaction mixture.

Electron Microscopy

Mitochondria were transferred to a sucrose solution containing 3 mM PQ, 2 mM NADH, 5 μM rotenone, 1 μM *p*-hydroxymercuribenzoate, and the solution was reacted for 30 min at 37 °C (11, 12). Superoxide dismutase (SOD; 3000 units/ml, Sigma-Aldrich) effects were evaluated by the addition of SOD to the reaction mixture. Anti-VDAC1 mAb (3 μg/ml) effects were evaluated by preincubation with the mitochondria for 5 min at 37 °C. The reaction was stopped by the addition of cold buffer. Mitochondria were immediately centrifuged, and the packed sediments were covered with 2% glutaraldehyde in phosphate-buffered saline and fixed for 1 h. The fixed clots were prepared for electron microscopy (11) and then observed by a transmission electron microscope (JEM-1200EX, JEOL Co. Ltd, Tokyo, Japan). The percentage of intact mitochondria per area was counted, and the mean of three areas was calculated.

Growth Inhibition Assays

Growth inhibition assays were performed by the stepwise addition of PQ, according to the method described by Saotome (20). Subconfluent HeLa cells were harvested by trypsinization and were precultured on 96-well plates (3×10^3 cells per well) for 24 h. Cells were treated with 7–250 μM PQ and were then cultured for 72 h. The effects of Trolox® (a water-soluble analog of vitamin E; 1 mM, Sigma-Aldrich) were evaluated by its addition to the medium. The 50% growth inhibition toxicity (IC_{50}) was estimated at 72 h.

Extraction of NADH-PQ Oxidoreductase from the Outer Membrane

To extract NADH-PQ oxidoreductase, two-step extraction with Triton X-100, deoxycholate followed by SDS/Igepal® CA-630 was performed (21). The outer membranes were isolated from the mitochondria by discontinuous sucrose gradient centrifugation (12). The isolated outer membranes were suspended in 20 mM Tris-HCl buffer (pH 7.6) containing 1% Triton X-100, 1% sodium deoxycholate, and 1 mM EDTA. The suspensions were left to stand on ice for 1 h. Suspensions were then centrifuged at 105,000 × *g* for 60 min. The precipitates were resuspended in a 20 mM Tris buffer with 0.06% SDS and 0.1% Igepal CA-630. The suspensions were left on ice for 1 h. The supernatants were collected by centrifugation at 105,000 × *g*.

Preparation of NADH-PQ Oxidoreductase Fraction

The supernatants were diluted with 20 mM Tris-HCl buffer (pH 8.0) containing 0.03% Triton X-100 and 10% glycerol, and the dilutions were loaded onto an anion exchange column (DEAE MemSep® 1000; Millipore Corp. Billerica, MA). The columns were washed with the Tris buffer, and proteins were eluted using a NaCl gradient. The fractions containing NADH-PQ oxidoreductase were collected from 0.25–0.3 M

NaCl fractions and dialyzed against a 20 mM Tris-HCl buffer (pH 7.6) containing 0.03% Triton X-100 and 10% glycerol.

Assays of NADH-PQ Oxidoreductase Activity

NADH Oxidation—The extracts were incubated with 0.2 mM NADH in Tris-buffered saline (TBS) containing 5 μM rotenone and 1 μM *p*-hydroxymercuribenzoate at 37 °C followed by the addition of 10 mM PQ. Activities were calculated by the first-order velocity of NADH oxidation measured at $\lambda_{340\ nm}$ ($e = 6.3 \times 10^3\ M^{-1}cm^{-1}$).

O_2^- Production—O_2^- production by NADH-PQ oxidoreductase activity was assayed using a Diogenes® luminescence system (National Diagnostics Inc., Atlanta, GA). The extracts were mixed with NADH (0.1 mM), PQ (0.0012–5 mM), and Diogenes (3-fold dilution) in TBS on a 384-well plate. The effects of DIDS (100 μM) and anti-VDAC1 mAb (30 μg/ml) were evaluated by the addition of these reagents to the mixture. The total volume of the reaction mixture was 15 μl. Chemiluminescence produced by superoxide was detected by an Envision® multilabel plate reader (PerkinElmer Life Sciences).

Immunoprecipitation

The extracts were incubated with anti-VDAC1 mAb or normal mouse IgG as a control. After incubation in TBS for 90 min at 4 °C, Protein A slurries (Amersham Biosciences) were added to the solution and gently stirred for 90 min at 4 °C. The suspensions were centrifuged, and the supernatants were obtained for the assay.

Zymography and Western Blot Analysis

The NADH-PQ oxidoreductase fraction was mixed with 0.125 M Tris-HCl buffer (pH 6.8) containing 20% glycerol and 0.02% bromphenol blue (1:1, v/v), and the mixture was loaded on native-polyacrylamide gel (5–10% gradient gel; Funakoshi, Tokyo, Japan). Electrophoresis was performed at 5 mA for 5 h on ice, and the gel was immersed in 20 mM Tris-HCl buffer (pH 7.4) containing 20% glycerol, 0.25 mM nitro blue tetrazolium, 5 μM rotenone, and 1 μM *p*-hydroxymercuribenzoate. The gel was incubated with 2 mM NADH and 10 mM PQ at room temperature for 30 min and washed with TBS, and the active bands were stained by diformazan. The electrophoresed gel was blotted, and detection was performed with anti-VDAC1 mAb. Additionally, the active band was excised and subjected to SDS-PAGE followed by Western blot analysis with anti-VDAC1 mAb.

Synthesis of Biotinylated PQ

The biotinylated paraquat was synthesized in moderate yield by condensation reaction of (+)-biotin and 3-(1′-methyl-4,4′-bipyridinium)propylammonium salt, which was prepared by successive *N*-alkylation of 4,4′-bipyridine with iodomethane and 3-bromopropylamine hydrobromide. See the supplemental methods for detailed procedures.

Plasmid Construction

Human *vdac1* cDNA was isolated as an XhoI fragment by PCR and was subcloned into pUC-CAGGS expression vector (22).

Synthesis of VDAC1 Protein Using a Cell-free Protein Synthesis System

The cDNA of VDAC1 was used. For wheat cell-free protein production of VDAC proteins, the VDAC DNA templates were constructed by "split-primer" PCR (23). The first round of PCR was performed on the cDNA using 10 nM concentrations of each of the following primers: a specific primer (5′-CCACCCACCACCACCAATGGCTGTGCCACCCACGT and AODA2306 primer, 5′-AGCGTCAGACCCCGTAGAAA). Then a second round of PCR was carried out to construct the templates for protein synthesis using a portion (5 μl) of the first PCR mix: 100 nM SPu primer (5′-GCGTAGCATTTAGGTGACACT), 100 nM AODA2303 primer (5′-GTCAGACCCCGTAGAAAAGA), and 1 nM deSP6E02 (5′-GGTGACACTATAGAACTCACCTATCTCTCTACACAAAACATTTCCCTACATACAACTTTCAACTTCCTATTCCACCCACCACCACCAATG). Wheat cell-free protein synthesis of VDAC protein was carried out using a robotic synthesizer (24, 25), GenDecorder1000® (CellFree Sciences, Yokohama, Japan) as described below. First, the transcript was created from each of the DNA templates mentioned above using SP6 RNA polymerase. The synthetic mRNAs were then precipitated with ethanol and collected by centrifugation using a Hitachi R10H rotor. Each mRNA (usually 30–35 μg) was washed and transferred into a translation mixture. The translation reaction was performed in the bilayer mode (26) with slight modifications. The translation mixture that formed the bottom layer consisted of 60 A260 units of wheat germ extract (CellFree Sciences) and 2 μg of creatine kinase (Roche Diagnostics) in 25 μl of SUB-AMIX® (CellFree Sciences). The SUB-AMIX® contained (final concentrations) 30 mM Hepes/KOH at pH 8.0, 1.2 mM ATP, 0.25 mM GTP, 16 mM creatine phosphate, 4 mM dithiothreitol, 0.4 mM spermidine, 0.3 mM concentrations of each of the 20 amino acids, 2.7 mM magnesium acetate, and 100 mM potassium acetate. 125 μl of the SUB-AMIX was placed on the top of the translation mixture, forming the upper layer. After incubation at 26 °C for 17 h, the synthesized proteins were confirmed by SDS-PAGE.

Binding Assay

The synthesized VDAC1 protein was mixed with biotinylated PQ (0–1.0 μM) in TBS containing 10% EZ block (Atto Corp., Tokyo, Japan) for 1 h. The mixtures were added to Nunc Immobilizer® streptavidin plates (Nunc, Roskilde, Denmark), which were incubated for 2 h. The plates were then washed with TBS containing 0.1% Tween 20 (TTBS). VDAC1 protein bound to biotinylated PQ was detected by anti-VDAC1 mAb (Calbiochem) followed by the addition of horseradish peroxidase-conjugated second antibody. ECL plus® (GE Healthcare) was used as a substrate of horseradish peroxidase. For NADH binding assay, biotinylated NAD^+ (R&D Systems, Inc., Minneapolis, MN) was mixed with outer membrane extract, and serial dilutions of non-labeled NADH were added for 1 h. The mixtures were incubated with anti-VDAC1 mAb, which was immobilized on Nunc Immobilizer 96-well plates in 10% EZ block (Atto Corp) for 2 h. The plates were washed with TTBS to which ExtrAvidin® peroxidase (Sigma) was added followed by a wash

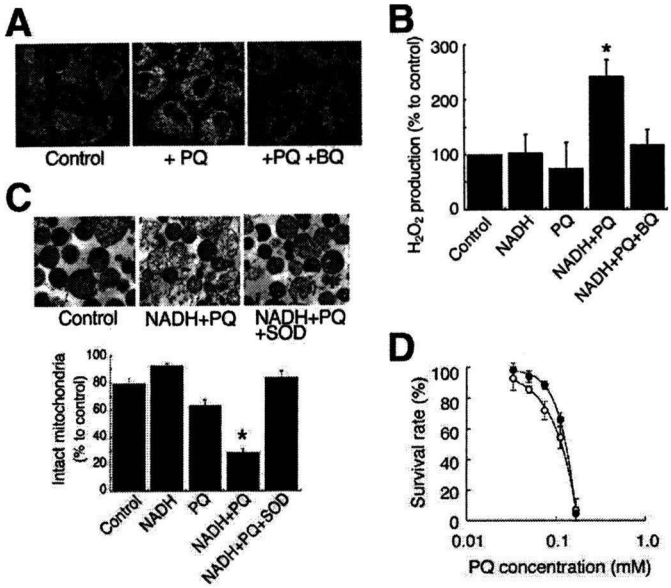

FIGURE 1. **Damage to mitochondria caused by NADH-dependent O_2^- production induced by PQ.** *A*, mitochondrial O_2^- production was visualized by MitoSOX in cells treated with PQ (1 mM) and BQ (0.2 mM). *B*, H_2O_2 production in isolated mitochondria was estimated by DCF florescence method. Mitochondria were incubated with 10 mM PQ, 2 mM NADH, and 0.3 mM BQ (*, $p < 0.01$, *versus* control). *C*, isolated mitochondria were incubated with 3 mM PQ, 2 mM NADH, and the 3000 IU/ml SOD. *Upper panels*, electron micrograph. *Lower graph*, percentages of intact mitochondria (*, $p < 0.001$, *versus* control). *D*, the survival rate of HeLa cells exposed to PQ (*open circle*) and PQ and 1 mM Trolox® (*closed circle*). Each point is the average of two to four experiments. *Error bars* represent S.E.

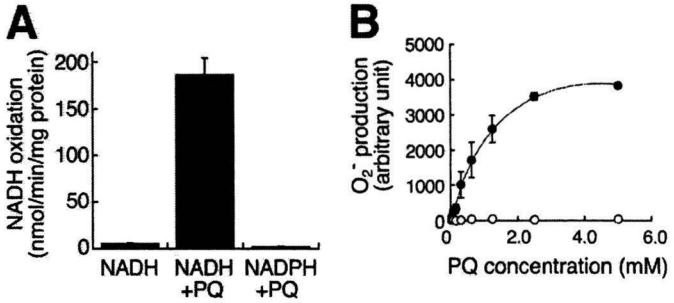

FIGURE 2. **NADH-PQ oxidoreductase activity in the outer membrane extract.** *A*, NADH (0.2 mM) was oxidized by the outer membrane extract in the presence of PQ (5 mM), but NADPH (0.2 mM) was not oxidized. *B*, PQ dose-dependent relationship to O_2^- production activity was observed by co-administration with NADH (0.1 mM) to the outer membrane extract (*closed circle*). In contrast, NADPH (0.1 mM) did not exert any such PQ effects (*open circle*). All *error bars* represent S.D. ($n = 3$).

with TTBS. ECL plus was used for the detection of binding. Immobilized normal mouse IgG was used as a control.

DNA Transfection

HeLa cells were transfected with the VDAC1 plasmid using Effectene® (Qiagen GmbH, Hilden, Germany).

Small Interfering RNA (siRNA) Transfection

HeLa cells were transfected for 72 h with 5 nM control siRNA or Hs_VDAC1_1HP_siRNA (Qiagen) using HiPerFect® transfection reagent (Qiagen).

Statistics

Statistical analyses were conducted using analysis of variance for multiple comparisons and Student's *t* test for comparing two groups.

RESULTS

PQ Produces O_2^- in an NADH-dependent Manner—We first investigated whether PQ produced ROS on mitochondria in HeLa cells. We detected O_2^- on the mitochondria using MitoSOX fluorogenic dye (Fig. 1*A*). Whereas only slight fluorescence was detected on the mitochondria in cells exposed to normal conditions, highly intense levels of fluorescence were observed when the cells were exposed to PQ. Fluorescence was reduced to the control level with the addition of BQ, a scavenger of O_2^-. In isolated rat liver mitochondria, we detected the NADH-dependent production of H_2O_2 by PQ using DCFH fluorescent dye (Fig. 1*B*). Although the fluorescence intensity did not change when PQ or NADH alone was added to the isolated mitochondria, the addition of PQ in combination with NADH raised the intensity of fluorescence in the mitochondria. BQ suppressed this augmentation. We also observed that the co-administration of PQ and NADH led to a loss of structural integrity of the isolated mitochondria, and SOD suppressed this damage (Fig. 1*C*). Furthermore, Torolox®, an O_2^- scavenger, significantly increased the survival rates of HeLa cells exposed to PQ ($p < 0.05$, Fig. 1*D*). These results indicated that PQ produced O_2^- in an NADH-dependent manner in mitochondria and damaged mitochondria followed by cell death.

VDAC1 Is Responsible for NDAH-PQ Oxidoreductase Activity—To reveal the components involved in this activity, we performed two-step extraction with Triton X-100, deoxycholate followed by SDS/Igepal CA-630 from the outer membrane and analyzed SDS/Igepal extract. The extract oxidized NADH, but not NADPH, by the addition of PQ (Fig. 2*A*), and O_2^- was produced in a PQ dose-dependent manner (Fig. 2*B*). The NADH oxidation activity was 4.4 times that of the Triton X-100/deoxycholate extract (data not shown). To ascertain whether or not VDAC protein is involved in NADH-PQ oxidoreductase activity, we examined the effects of VDAC inhibitors on this activity (Fig. 3*A*). O_2^- production by the extract from the outer membrane mixed with PQ and NADH was significantly inhibited by DIDS, an anion channel inhibitor, or anti-VDAC1 mAb, but such inhibition was not observed with exposure of the extract to normal mouse IgG. When the extract was immunoprecipitated with anti-VDAC1 mAb, the activity in the supernatant was lower than that observed with the administration of normal IgG (Fig. 3*B*). Furthermore, we confirmed that DIDS and anti-VDAC1 mAb inhibited the production of O_2^- and also inhibited the breakdown of isolated mitochondria exposed to PQ and NADH (Fig. 3, *C* and *D*). These results suggest that VDAC1 is responsible for NADH-PQ oxidoreductase activity.

VDAC1 Is Component of NADH-PQ Oxidoreductase—Because, VDAC1 protein was more highly concentrated in the SDS/Igepal extract than in the Triton X-100/deoxycholate extract (Fig. 4*A*), we investigated whether or not VDAC1 protein is contained in the oxidoreductase. We purified the active fraction from the SDS/Igepal extract using DEAE chromatography and carried out zymography on the fraction by native PAGE in blue tetrazolium solution with PQ and NADH. A

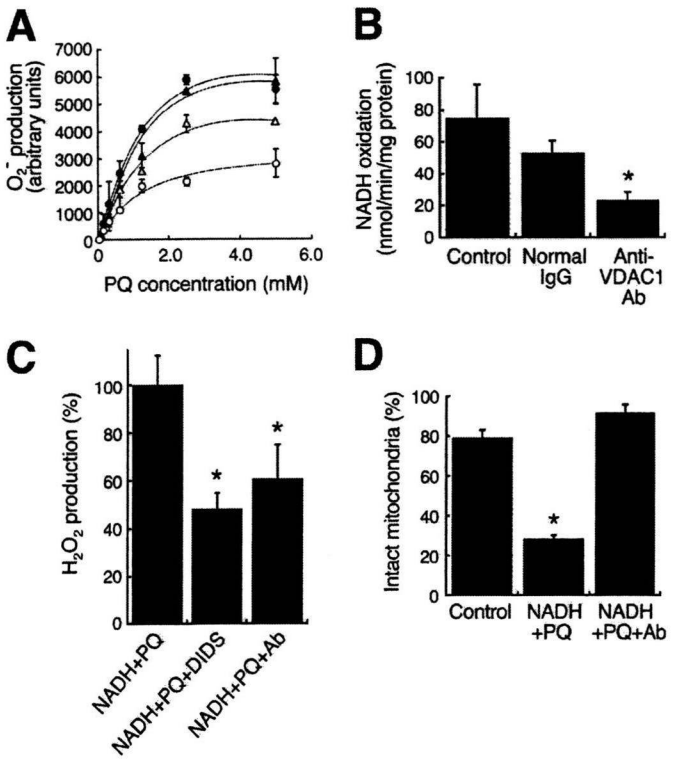

FIGURE 3. **Participation of VDAC1 in the NADH-PQ oxidoreductase activity and mitochondrial damage.** *A*, O_2^- production in the outer membrane extract (*closed circle*) was inhibited by DIDS (100 μM; *open circle*, $p < 0.001$, $n = 3$) and anti-VDAC1 mAb (30 μg/ml; *open triangle*, $p < 0.05$, $n = 3$). *Closed triangle*, treated with normal IgG (30 μg/ml). *Error bars* represent S.D. ($n = 3$). *B*, the extract was immunoprecipitated with anti-VDAC1 mAb or normal IgG, and the NADH-oxidation activity of the supernatants was measured. *Control*, no treatment. *, $p < 0.01$, *versus* control. *Error bars* represent S.D. ($n = 3$). *C*, H_2O_2 production in isolated mitochondria by PQ (10 mM) co-administered with NADH (2 mM) was estimated by DCF florescence method. DIDS (100 μM) and anti-VDAC1 mAb (9 μg/ml) were inhibited H_2O_2 production. *, $p < 0.001$ with respect to the control. Each point is the mean of triplicate experiments. *Error bars* represent S.E. *D*, effects of anti-VDAC1 antibody on the NADH-PQ-dependent breakage of mitochondria were estimated. Isolated mitochondria were ruptured by the co-administration of PQ (3 mM) and NADH (2 mM), whereas the addition of anti-VDAC1 mAb (9 μg/ml) protected the mitochondria from such breakage. *, $p < 0.01$ *versus* the control. Each point is the mean of triplicate experiments. *Error bars* represent S.E.

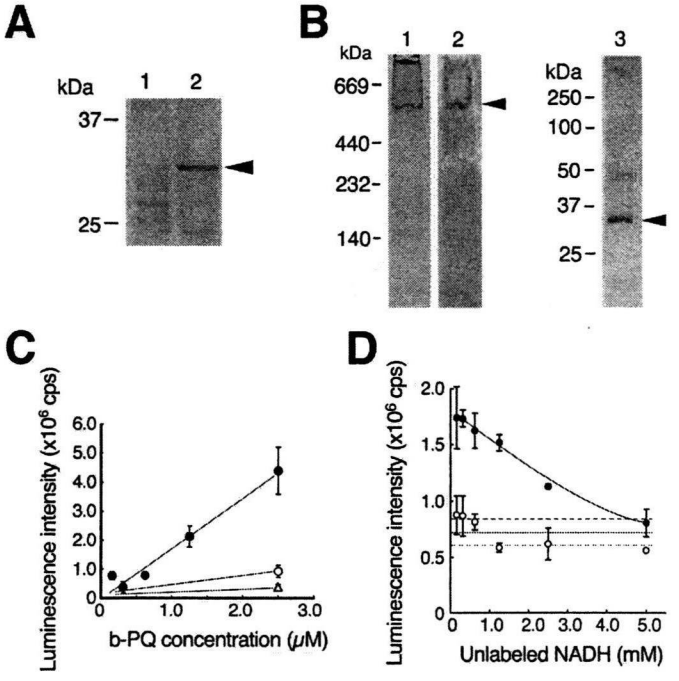

FIGURE 4. **VDAC1 is a component of NADH-PQ oxidoreductase.** *A*, extracts obtained from the mitochondrial outer membrane by treatment with Triton X-100/deoxycholate (*lane 1*) or SDS/ Igepal CA-630 (*lane 2*) were run on SDS-PAGE, and the results were analyzed by Western blotting with anti-VDAC1 mAb. VDAC1 protein was detected by the mAb (*arrowhead*). *B*, DEAE fractions from the extracts containing oxidoreductase activity were examined by zymography with NADH and PQ in blue tetrazolium solution (*lane 1*). The active band was consistent with the anti-VDAC1 mAb-detected band (*lane 2*, *arrowhead*), and this band was excised and subjected to Western blot analysis using anti-VDAC1 mAb (*lane 3*; the *arrowhead* indicates VDAC1 protein). *C*, direct binding to VDAC1 was assayed using biotinylated (*b-*) PQ (*closed circle*) in competition with non-labeled PQ (*open circle*, 25 μM, *open triangle*, 250 μM). *Error bars* represent S.D. ($n = 3$). *D*, assay of NADH binding to the outer membrane extracts was performed. The extracts were trapped by immobilized anti-VDAC1 antibody and incubated with biotinylated NAD^+. Bound biotinylated NAD^+ was reduced by exposure to non-labeled NADH ($p < 0.01$, *closed circles*). When normal IgG was used for trapping, no NADH competition was detected (*open circles*). *Broken lines* represent 95% confidence interval of the control value. *Error bars* represent S.D. ($n = 3$).

major reactive band stained with dark blue diformazan, a form of blue tetrazolium reduced by O_2^-, appeared at 500 kDa (Fig. 4*B*, *lane 1*); this band was recognized using anti-VDAC1 mAb (*lane 2*). Next, the excised band was examined by Western blot analysis with SDS-PAGE using anti-VDAC1 mAb. The antibody recognized a band at 31 kDa, the size of VDAC1 (*lane 3*). Because several proteins were detected in the reactive band by SDS-PAGE followed by silver staining (data not shown), the oxidoreductase may be a complex containing the VDAC1 protein. To confirm the direct interaction of VDAC1 with PQ, we performed a binding assay using recombinant VDAC1 protein and biotinylated PQ (Fig. 4*C*). We detected biotinylated PQ dose-dependently bound to the VDAC1 protein, and excess non-labeled PQ competed for the binding. Next, we examined the interaction of VDAC1 with NADH using biotinylated NAD^+. Whereas the biotinylated NAD^+ was not found to bind to the recombinant VDAC1 protein, which was immobilized by anti-VDAC1 mAb (data not shown), we did detect binding of the biotinylated NAD^+ using the SDS/Igepal extract instead of the VDAC1 protein (Fig. 4*D*). These results were compatible with the absence of NADH-PQ oxidoreductase activity in the recombinant VDAC1 protein or purified VDAC from rat liver mitochondria (data not shown). The present results indicate that VDAC1 is involved in NADH-PQ oxidoreductase activity as a component of the PQ binding site.

VDAC1 Is Responsible for the Cytotoxicity of PQ—Finally, we determined whether the amount of VDAC1 protein in cells affects PQ sensitivity. We obtained stable transfectants of HeLa cells overexpressing VDAC1; these cells had 2.2 times the VDAC1 protein content of control cells (Fig. 5*A*). When treated with PQ, these VDAC1-overexpressing cells showed 2.0 times the intracellular production of H_2O_2 compared with that of control cells (Fig. 5*B*). The IC_{50} of control cells exposed to PQ was 72.3 μM, and this value fell to 30.7 μM in the VDAC1-overexpressing cells (Fig. 5*C*). When HeLa cells were transfected with VDAC1 siRNA, almost no VDAC1 protein was synthesized (Fig. 6*A*). Mitochondria were isolated from these cells, and the NADH-PQ dependent H_2O_2 production was estimated (Fig. 6*B*). The production of H_2O_2 on the mitochondria from knockdown cells was reduced to endogenous levels. The sur-

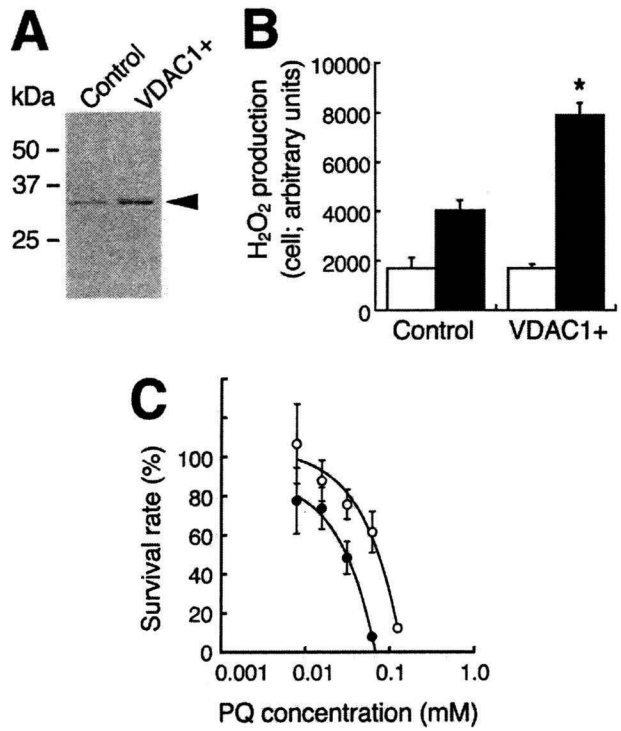

FIGURE 5. **Effects of VDAC1 overexpression on the PQ-dependent H_2O_2 production and the cytotoxicity in HeLa cells.** *A*, lysates from VDAC1-overexpressing cells were subjected to Western blot analysis with anti-VDAC1 mAb. *Control*, cells transfected with empty vector; *VDAC+*, cells transfected with the vector bearing *vdac1* cDNA. *B*, H_2O_2 production by PQ in VDAC1-overexpressing cells (*VDAC1+*) was higher than that of control cells (*, $p < 0.001$). *Light bars*, no treatment; *dark bars*, exposure to 1 mM PQ. *Error bars* represent S.D. ($n = 3$). *C*, the survival rates of VDAC1-overexpressing HeLa cells (*closed circle*) were lower than those of controls (open circle; $p < 0.001$). *Error bars* represent S.E. of triplicate experiments.

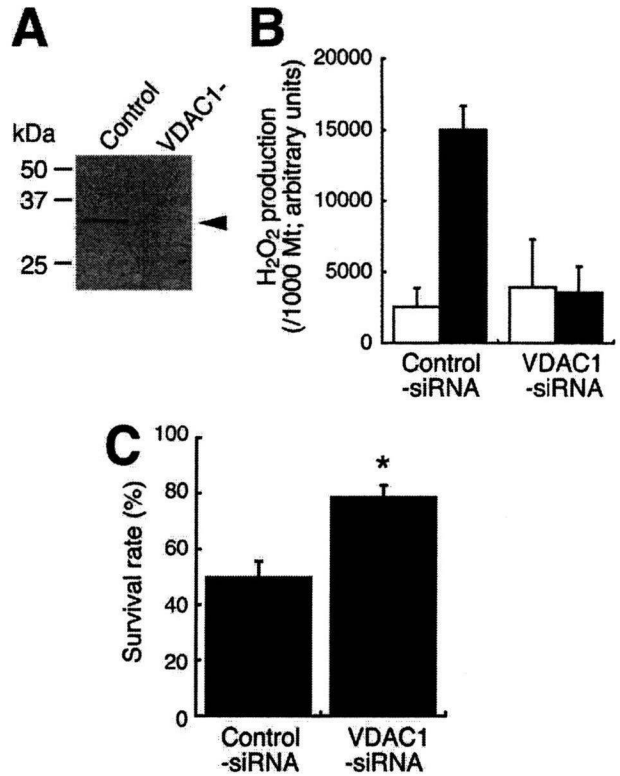

FIGURE 6. **Effects of VDAC1 knockdown on the PQ-dependent H_2O_2 production and the cytotoxicity in HeLa cells.** *A*, lysates from knockdown cells were subjected to Western blot analysis with anti-VDAC1 mAb. *Control*, cells transfected with the control siRNA; *VDAC−*, cells transfected with VDAC1 siRNA. The *arrowheads* indicate VDAC1 protein. *B*, NADH-PQ-dependent H_2O_2 production on mitochondria isolated from VDAC1-knockdown HeLa cells was estimated by DCF assay. *Light bars*, mitochondria incubated with 2 mM NADH only; *dark bars*, mitochondria were incubated with 10 mM PQ and 2 mM NADH. *Error bars* represent S.D. ($n = 3$). *C*, the survival rate of VDAC1-knockdown HeLa cells (VDA1-siRNA) after 24 h of exposure to 222 μM PQ was higher than that of control cells ($p < 0.001$). *Error bars* represent S.E. of triplicate experiments.

vival rate after exposure of the VDAC1 knockdown cells to 222 μM PQ for 24 h was 79% compared with 50% in controls (Fig. 6*C*). These results indicated that VDAC1 is responsible for the cytotoxicity of PQ as an NADH-dependent oxidoreductase.

DISCUSSION

In this study we demonstrate that a mitochondrial system, not a microsomal system, is involved in PQ poisoning; PQ produces O_2^- by NADH-dependent oxidoreductase in the outer membrane of mitochondria and damages mitochondria, leading to cell death. Furthermore, we present that mitochondrial VDAC1 is responsible for this activity as a component of the PQ binding site.

We observed O_2^- production on the mitochondria after administering PQ to cells using MitoSOX, an O_2^--specific fluorescent dye. Additionally, we detected H_2O_2 production on isolated mitochondria in the presence of PQ and NADH using DCFH fluorescent dye, and BQ reduced the level of production. In a previous study we observed that cytochrome *c*, an O_2^- scavenger, diminished H_2O_2 production on mitochondria incubated with PQ and NADH (13). Because O_2^- is immediately (10^5 $M^{-1}s^{-1}$) converted into H_2O_2 in aqueous solution, DCF fluorescence demonstrating H_2O_2 is considered to be equivalent to a demonstration of O_2^- production (13). We also indicated that PQ destroyed isolated mitochondria in the presence of NADH and that SOD suppressed this damage. Furthermore, Trolox® suppressed the toxicity of PQ in cells. We formerly reported that PQ selectively destroyed the mitochondria of pulmonary type II cells and hepatocyte *in vivo* (6, 11) and also destroyed cultured type II cells (7). These results indicate that PQ attacks mitochondria by NADH-dependent O_2^- production in the course of its cytotoxicity.

In an ultrastructural study, we previously observed that NADH-dependent O_2^- production by PQ occurred in the outer membrane of mitochondria (13) and demonstrated that the NADH oxidation activity by PQ in the outer membrane fraction was five times that of the inner membrane fraction (12). O_2 uptake on mitochondria took place with the addition of PQ and NADH (11, 12), and blue PQ radicals formed under anaerobic conditions (11). In the present study we again observed NADH oxidation and PQ radical formation in the outer membrane under anaerobic conditions (data not shown). These results indicated that an NADH-PQ oxidoreductase is localized in the outer membrane. We previously confirmed that NADH-cytochrome b_5 reductase, an outer membrane-localized oxidoreductase, did not participate in the PQ reduction, based on its insensitivity to anti-NADH-cytochrome b_5 reductase antibody and a different sensitivity to *p*-hydroxymercuribenzoate (12). We also reported that rotenone, an inhibitor of complex I in the electron

transport chain, did not inhibit NADH-dependent PQ reduction (11, 12). Intriguingly, we find that VDAC1 is a constituent of the NADH-PQ oxidoreductase. VDAC1 is a small, abundant, pore-forming protein found in the outer membranes of all eukaryotic mitochondria and plays an important role in the passage of adenine nucleotides, Ca^{2+}, and other metabolites through the outer membrane (27). In addition, VDAC1 located at contact sites between the outer and inner membranes forms permeability transition pores (PTPs) with the adenine nucleotide transporter, cyclophilin D, and other proteins (27). It is unknown whether PTP proteins besides VDAC1 participate in the NADH-PQ oxidoreductase activity; thus, it will still be necessary to investigate their involvement with PTP proteins.

Extramitochondrial oxidative stress induces PTP openings via VDAC protein without damage to the inner membrane (27). PQ does not penetrate mitochondrial membrane (28), and $O_2^{\cdot-}$ production by PQ occurs on the outer surface of the outer membrane (13). Furthermore, we demonstrated the binding of PQ to VDAC1 protein by biotinylated PQ and the inhibition of PQ-dependent mitochondrial breakage by anti-VDAC1 mAb. These results indicated that the breakage of mitochondria by PQ occurred through VDAC1. The binding mechanism of PQ, a cation molecule, to VDAC1 remains unknown. It has been reported that NADH increased the voltage dependence of VDAC and reduced the conductance of the outer membrane (29, 30). The ion selectivity of VDAC changed from anions to cations when conductance decreased (31). NADH may, therefore, affect the binding of PQ to VDAC1. Baker *et al.* (16) reported that VDAC1 localized in the plasma membrane functions as NADH-ferricyanide reductase and that VDAC1 has a putative NAD^+ binding motif. Yehezkel *et al.* (32) demonstrated that VDAC purified from rat liver mitochondria had nucleotide binding sites bound to ATP; however, NADH did not bind them. As in a previous study (Hirai *et al.* (11), the change in conformation from the orthodox to the condensed type occurred when NADH was added to starved intact mitochondria. In addition, NADH reduced the permeability of the outer membrane to ADP (15). These results indicated that NADH affects PTP even though NADH does not bind to VDAC1 directly. Although we did not observe the direct binding of NADH to VDAC1 alone, we did observe the binding of biotinylated NAD^+ to the NADH-PQ oxidoreductase concentrated extract, which was trapped by anti-VDAC1 mAb. NADH-PQ oxidoreductase activity was inhibited by DIDS and anti-VDAC1 mAb, but recombinant VDAC1 protein or purified VDAC protein alone had no activity. Therefore, an NADH binding component is expected to be necessary to yield this activity.

Yagoda *et al.* (33) reported that VDAC2 or VDAC3 was implicated in the cytotoxicity of the anti-tumor agent erastin, which was shown to induce oxidative cell death; in particular, VDAC2 was found to bind directly to this agent. We have not yet identified the involvement of VDAC2 or VDAC3 in NADH-PQ oxidoreductase activity. It has been reported that VDAC1 is the most abundantly expressed of the three VDAC isoforms in mammalian mitochondria (34). In addition, we demonstrated a correlation between the production of $O_2^{\cdot-}$ and VDAC1 expression, and we observed defective $O_2^{\cdot-}$ production on the mitochondria isolated from VDAC1 knockdown cells. Therefore, it appears that VDAC1 participates primarily in NADH-PQ oxidoreductase activity. Recently, we found that several furanonaphthoquinones caused mitochondrial damage and the apoptosis of cancer cells by the production of ROS, and other studies revealed that VDAC1 induces ROS production by an NADH-dependent quinone reduction (17, 35). Additionally, we previously demonstrated that menadione, a naphthoquinone, was a substrate of NADH-PQ oxidoreductase (12). These previous and present results taken together suggest that the function of VDAC1 is not only to serve as a channel but also to function as part of an oxidoreductase enzyme.

Until now, management of PQ poisoning has been directed primarily at removing PQ from the gastrointestinal tract by the use of several absorbents (activated charcoal, Fuller's Earth, etc.) and increasing its excretion from the blood by hemoperfusion (2). However, the efficacy of these treatments is poor. Our results indicated that $O_2^{\cdot-}$ production by a VDAC-containing mitochondrial system is responsible for PQ poisoning. DIDS and anti-VDAC1 antibody inhibited NADH-PQ oxidoreductase activity, mitochondrial $O_2^{\cdot-}$ production, and the breakage of mitochondria by PQ. Furthermore, PQ cytotoxicity was suppressed in VDAC1-knockdown cells. These results suggest that specific VDAC inhibitors can be therapeutic agents of PQ poisoning.

Acknowledgment—We are grateful to Mayumi Mitani for secretarial assistance.

REFERENCES

1. Wesseling, C., van Wendel de Joode, B., Ruepert, C., León, C., Monge, P., Hermosillo, H., and Partanen, T. J. (2001) *Int. J. Occup. Environ. Health* **7**, 275–286
2. Dinis-Oliveira, R. J., Duarte, J. A., Sánchez-Navarro, A., Remião, F., Bastos, M. L., and Carvalho, F. (2008) *Crit. Rev. Toxicol.* **38**, 13–71
3. McCormack, A. L., Thiruchelvam, M., Manning-Bog, A. B., Thiffault, C., Langston, J. W., Cory-Slechta, D. A., and Di Monte, D. A. (2002) *Neurobiol. Dis.* **10**, 119–127
4. Baldwin, R. C., Pasi, A., MacGregor, J. T., and Hine, C. H. (1975) *Toxicol. Appl. Pharmacol.* **32**, 298–304
5. Bus, J. S., Cagen, S. Z., Olgaard, M., and Gibson, J. E. (1976) *Toxicol. Appl. Pharmacol.* **35**, 501–513
6. Hirai, K., Witschi, H., and Côté, M. G. (1985) *Exp. Mol. Pathol.* **43**, 242–252
7. Wang, G. Y., Hirai, K., and Shimada, H. (1992) *J. Electron Microsc. (Tokyo)* **41**, 181–184
8. Yang, W., and Tiffany-Castiglioni, E. (2005) *J. Toxicol. Environ. Health A* **68**, 1939–1961
9. St. Clair, D. K., Oberley, T. D., and Ho, Y. S. (1991) *FEBS Lett.* **293**, 199–203
10. Oliver, P. D., and Newsome, D. A. (1992) *Invest. Ophthalmol. Vis. Sci.* **33**, 1909–1918
11. Hirai, K., Ikeda, K., and Wang, G. Y. (1992) *Toxicology* **72**, 1–16
12. Shimada, H., Hirai, K., Simamura, E., and Pan, J. (1998) *Arch Biochem. Biophys* **351**, 75–81
13. Hirai, K. I., Pan, J., Shimada, H., Izuhara, T., Kurihara, T., and Moriguchi, K. (1999) *J. Electron Microsc. (Tokyo)* **48**, 289–296
14. Shimada, H., Furuno, H., Hirai, K., Koyama, J., Ariyama, J., and Simamura, E. (2002) *Arch. Biochem. Biophys.* **402**, 149–157
15. Lee, A. C., Xu, X., and Colombini, M. (1996) *J. Biol. Chem.* **271**, 26724–26731
16. Baker, M. A., Lane, D. J., Ly, J. D., De Pinto, V., and Lawen, A. (2004) *J. Biol. Chem.* **279**, 4811–4819

17. Simamura, E., Hirai, K., Shimada, H., Koyama, J., Niwa, Y., and Shimizu, S. (2006) *Cancer Biol. Ther.* **5,** 1523–1529
18. Ariyama, J., Shimada, H., Aono, M., Tsuchida, H., and Hirai, K. I. (2000) *Intensive Care Med.* **26,** 981–987
19. Nakayama, S., Sakuyama, T., Mitaku, S., and Ohta, Y. (2002) *Biochem. Biophys. Res. Commun.* **290,** 23–28
20. Saotome, K., Morita, H., and Umeda, M. (1989) *Toxicol. In Vitro* **3,** 317–321
21. Teraoka, K., and Matsui, S. (1999) *Nippon Rinsho.* **57,** (suppl.) 784–788
22. Narita, M., Shimizu, S., Ito, T., Chittenden, T., Lutz, R. J., Matsuda, H., and Tsujimoto, Y. (1998) *Proc. Natl. Acad. Sci. U.S.A.* **95,** 14681–14686
23. Sawasaki, T., Ogasawara, T., Morishita, R., and Endo, Y. (2002) *Proc. Natl. Acad. Sci. U.S.A.* **99,** 14652–14657
24. Sawasaki, T., Kamura, N., Matsunaga, S., Saeki, M., Tsuchimochi, M., Morishita, R., and Endo, Y. (2008) *FEBS Lett.* **582,** 221–228
25. Sawasaki, T., Gouda, M. D., Kawasaki, T., Tsuboi, T., Tozawa, Y., Takai, K., and Endo, Y. (2005) *Methods Mol. Biol.* **310,** 131–144
26. Sawasaki, T., Hasegawa, Y., Tsuchimochi, M., Kamura, N., Ogasawara, T., Kuroita, T., and Endo, Y. (2002) *FEBS Lett.* **514,** 102–105
27. Crompton, M. (1999) *Biochem. J.* **341,** 233–249
28. Gage, J. C. (1968) *Biochem. J.* **109,** 757–761
29. Lee, A. C., Zizi, M., and Colombini, M. (1994) *J. Biol. Chem.* **269,** 30974–30980
30. Zizi, M., Byrd, C., Boxus, R., and Colombini, M. (1998) *Biophys. J.* **75,** 704–713
31. Vyssokikh, M., and Brdiczka, D. (2004) *Mol. Cell. Biochem.* **256–257,** 117–126
32. Yehezkel, G., Hadad, N., Zaid, H., Sivan, S., and Shoshan-Barmatz, V. (2006) *J. Biol. Chem.* **281,** 5938–5946
33. Yagoda, N., von Rechenberg, M., Zaganjor, E., Bauer, A. J., Yang, W. S., Fridman, D. J., Wolpaw, A. J., Smukste, I., Peltier, J. M., Boniface, J. J., Smith, R., Lessnick, S. L., Sahasrabudhe, S., and Stockwell, B. R. (2007) *Nature* **447,** 864–868
34. Yamamoto, T., Yamada, A., Watanabe, M., Yoshimura, Y., Yamazaki, N., Yoshimura, Y., Yamauchi, T., Kataoka, M., Nagata, T., Terada, H., and Shinohara, Y. (2006) *J. Proteome Res.* **5,** 3336–3344
35. Simamura, E., Shimada, H., Ishigaki, Y., Hatta, T., Higashi, N., and Hirai, K. I. (2008) *Anat. Sci. Int.* **83,** 261–266

Biosci. Biotechnol. Biochem., 73 (7), 1661–1664, 2009

Note

Construction of a Protein Library of Arabidopsis Transcription Factors Using a Wheat Cell-Free Protein Production System and Its Application for DNA Binding Analysis

Akira NOZAWA,[1,2] Yuko MATSUBARA,[1] Yoshinori TANAKA,[1] Hirotaka TAKAHASHI,[1] Tatsuya AKAGI,[1] Motoaki SEKI,[3] Kazuo SHINOZAKI,[4] Yaeta ENDO,[1,2,†] and Tatsuya SAWASAKI[1,2,†]

[1]*Cell-Free Science and Technology Research Center, and Venture Business Laboratory, Ehime University, 3 Bunkyo-cho, Matsuyama, Ehime 790-8577, Japan*
[2]*Systems and Structural Biology Center, RIKEN, 1-7-22 Suehiro-cho, Tsurumi-ku, Yokohama, Kanagawa 230-0045, Japan*
[3]*Plant Genomic Network Research Team, Plant Functional Genomics Research Group, RIKEN Plant Science Center, 1-7-22 Suehiro-cho, Tsurumi-ku, Yokohama, Kanagawa 230-0045, Japan*
[4]*Gene Discovery Research Team, Gene Discovery Research Group, RIKEN Plant Science Center, 3-1-1 Koyadai, Tsukuba, Ibaraki 305-0074, Japan*

Received January 9, 2009; Accepted February 19, 2009; Online Publication, July 7, 2009
[doi:10.1271/bbb.90026]

We created a protein library consisting of 647 Arabidopsis transcription factors (TFs) using a wheat cell-free system. The quality of proteins in the library was checked by binding assay of bZIP family proteins. Screening of TFs binding to 5′-regulatory regions of *FLC* and *LFY* was conducted using the library, and MYB67 and GBF1 were found to be binding factors.

Key words: Arabidopsis; wheat cell-free protein production system; transcription factor

The completion of entire genome sequences of various organisms has resulted in the identification of large numbers of novel genes.[1)] The challenge ahead is to gain information about the function of these novel genes. Currently, significant effort is devoted to understanding the roles of a gene by analyzing its expression pattern or by analyzing phenotypes of the gene-specific disruption mutant. In addition to this information, biochemical characterization of the protein encoded by the gene is essential for understanding its precise function. However, only slight progress has been made in the large-scale biochemical characterization of proteins, especially at the genome-wide level. To establish a proteomics approach for the characterization of proteins, it is necessary to meet three requirements, availability of i) a wide variety of proteins, ii) sufficient amounts of proteins, and iii) functionally folded proteins.

Transcription factors (TFs) play crucial roles in almost all biological processes. The Arabidopsis genome encodes more than 1,500 transcription factors.[2)] These TFs are classified into various TF families according to the distinct type of DNA binding domains, such as AP2/EREBP, bZIP, HD-ZIP, Myb, MADS, and several classes of zinc finger proteins. TFs control gene expression by binding to specific DNA sequences in the genome. However, the number of TFs whose binding sequences have been confirmed by biochemical analyses is limited, mainly because of the difficulty in obtaining sufficient amounts of purified TF proteins, as they are expressed in small quantities in the cell. Overexpression of recombinant TF proteins in cells is generally difficult because overexpression of TFs often inhibits host cell physiology. Here, we constructed an Arabidopsis TF protein library based on our wheat cell-free protein synthesis system.[3,4)] For evaluation of the library, we performed several biochemical analyses. Our results indicate that the cell-free based Arabidopsis TF protein library is a powerful tool in the large-scale functional analysis of TFs.

Genome analysis revealed at least 1,500 TFs, classifiable into 45 families, in the Arabidopsis genome.[2)] Out of these, cDNA clones of 1,076 TFs were in the RIKEN Arabidopsis full-length (RAFL) clone collection.[5)] *Escherichia coli* cells harboring the cDNA clones were inoculated individually in 96-well plates, and the plates were then incubated for 48 h at 37 °C. DNA templates for transcription were prepared from each *E. coli* clone using the split-primer polymerase chain reaction (PCR) method, as described in our previous reports.[4,6)] Finally, we prepared a total of 705 DNA templates for transcription from the 1,076 RAFL clones. mRNAs were prepared from each amplified DNA template, and the synthesized mRNAs were used for protein synthesis by the bilayer method.[7)] Following this protocol, we created a protein library, AtTF, consisting of 647 synthesized Arabidopsis TFs. The mean values for the amount (concentration) and solubility of all synthesized TFs were 1 μM and 72% respectively (Fig. 1A). The size of each protein synthesized was confirmed by SDS-polyacrylamide gel electrophoresis (PAGE) analysis (data not shown). We did not observe any major difference among the families as far as protein synthesis and solubility were concerned. All the families included both

† To whom correspondence should be addressed. Yaeta ENDO, Fax: +81-89-927-9941; E-mail: yendo@eng.ehime-u.ac.jp; Tatsuya SAWASAKI, Fax: +81-89-927-9941; E-mail: sawasaki@eng.ehime-u.ac.jp

Abbreviations: PAGE, polyacrylamide gel electrophoresis; RAFL, RIKEN Arabidopsis full-length; PCR, polymerase chain reaction; TF, transcription factor; TRR, transcription regulatory region

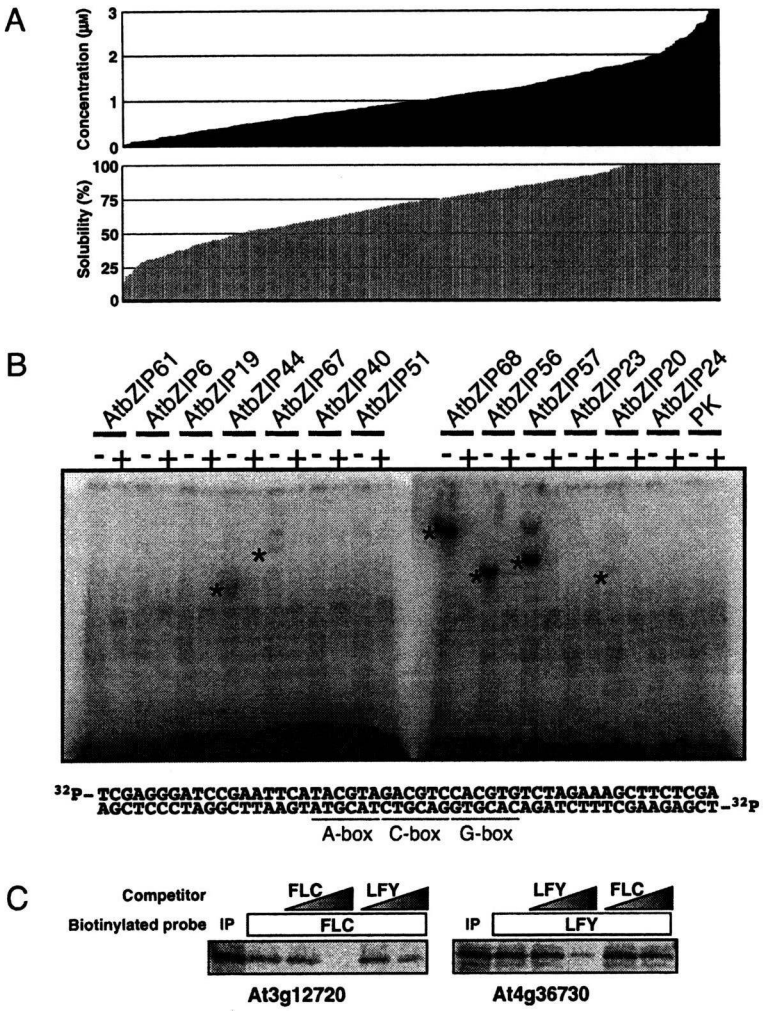

Fig. 1. Construction of a Protein Library of Arabidopsis Transcription Factors and Its Application to DNA Binding Assay.

A, High-throughput production of Arabidopsis TF proteins by the wheat germ cell-free protein synthesis system. Arabidopsis TF proteins (n = 647) were synthesized using the wheat germ cell-free system, as described in the text. The concentration (μM) and solubility of these synthesized TF proteins are shown in separate panels. Results are arrayed so that the value of each parameter increases from left to right in each panel. B, DNA binding analysis of the bZIP proteins. The [^{32}P]-labeled DNA probe (shown at the bottom of the figure) and an indicated bZIP protein were incubated in the presence (+) and the absence (−) of a competitor (10-fold excess of the non-labeled probe). After 30 min of incubation, the samples were subjected to PAGE. Asterisks indicate shifted bands of DNA-protein complex. Lanes of PK show results using a protein kinase, GSK1 (negative control). The nucleotide sequences of the oligonucleotides used as the probe are also shown. The sequences of the A-, C-, and G-boxes are underlined. C, Screening of TF proteins. TF proteins synthesized from cDNA clones (At3g12720 and At4g36730) were incubated with the respective biotinylated promoter probes in the presence and the absence of non-labeled competitor DNA fragment (*FLC* or *LFY*, 5- and 10-fold excess respectively). After 30 min, the samples were pulled down with streptavidin-conjugated magnetic beads, subjected to SDS–PAGE, and detected by autoradiography. IP, proteins inputted to this assay.

poorly-synthesized and well-synthesized TF proteins. There was no TF family from which no members could be synthesized using this cell-free protein synthesis system. These results suggest that our cell-free protein synthesis system can synthesize sufficient quantities of good-quality Arabidopsis TFs for functional analysis.

To determine whether these synthesized TF proteins can be used for functional analysis, we demonstrated two independent DNA binding assays using this protein library. First we examined the DNA binding activity of the bZIP TFs in this library. bZIP TFs have a basic region that binds to the DNA and a leucine zipper dimerization motif.[8] Proteins with bZIP domains are present in all eukaryotes analyzed to date. Some of the bZIP TFs, such as Jun/Fos or CREB, have been extensively studied in animals, and they serve as models for understanding TF-DNA interactions, ternary complex formation, and post-translational modifications.[8] Plant bZIP proteins bind to DNA sequences with an ACGT core, preferentially to A-box (TACGTA), C-box (GACGTC), and G-box (CACGTG).[9] Seventy-five bZIP transcription factors were found in the Arabidopsis genome, and they were classified into 11 groups.[8] In this study, 54 bZIP proteins were synthesized using the cell-free protein synthesis system. Among them, 45 bZIP proteins (60% of the family), concentration of which was approximately 0.4 μM, were used for the binding assay. The DNA-binding ability of each synthesized TF was detected by gel retardation assay using a specific DNA fragment that contained the A-, C-, and G-box. Gel retardation assay was conducted as previously described.[10] DNA-binding ability was confirmed for 19 out of 45 bZIPs proteins. The representative results of gel retardation assay are shown in Fig. 1B. The results of the DNA-binding assay are summarized in Table 1. bZIP proteins belonging to A, C, D, G, H, and S groups were reported to bind DNA sequences with an ACGT core.[8,11–14] Among them, binding of groups A,

Table 1. Results of DNA Binding Assay for the bZIP Family Proteins in Arabidopsis

Name	AGI code	G[a]	Published name	DNA binding	Name	AGI code	G	Published name	DNA binding
AtbZIP40	At1g03970	A	GBF4	nd[b]	AtbZIP68	At1g32150	G	.	YES
AtbZIP35	At1g49720	A	ABF1	YES	AtbZIP55	At2g46270	G	GBF3	YES
AtbZIP39	At2g36270	A	ABI5	nd	AtbZIP54	At4g01120	G	GBF2	YES
AtbZIP12	At2g41070	A	DPBF4	YES	AtbZIP41	At4g36730	G	GBF1	YES
AtbZIP67	At3g44460	A	DPBF2	YES	AtbZIP56	At5g11260	H	HY5	YES
AtbZIP66	At3g56850	A	AREB3	YES	AtbZIP69	At1g06070	I	.	nd
AtbZIP37	At4g34000	A	ABF3	YES	AtbZIP52	At1g06850	I	.	nd
AtbZIP13	At5g44080	A	.	nd	AtbZIP51	At1g43700	I	VIP1	nd
AtbZIP17	At2g40950	B	.	nd	AtbZIP59	At2g31370	I	PosF21	nd
AtbZIP28	At3g10800	B	.	nd	AtbZIP18	At2g40620	I	.	nd
AtbZIP25	At3g54620	C	.	nd	AtbZIP29	At4g38900	I	.	nd
AtbZIP9	At5g24800	C	BZO2H2	nd	AtbZIP44	At1g75390	S	.	YES
AtbZIP63	At5g28770	C	.	nd	AtbZIP2	At2g18160	S	GBF5	YES
AtbZIP22	At1g22070	D	TGA3	nd	AtbZIP6	At2g22850	S	.	nd
AtbZIP46	At1g68640	D	Perianthia	nd	AtbZIP53	At3g62420	S	.	YES
AtbZIP50	At1g77920	D	.	YES	AtbZIP11	At4g34590	S	GBF6	YES
AtbZIP20	At5g06950	D	TGA2	YES	AtbZIP3	At5g15830	S	.	YES
AtbZIP26	At5g06960	D	TGA5	YES	AtbZIP1	At5g49450	S	.	nd
AtbZIP57	At5g10030	D	TGA4	YES	AtbZIP62	At1g19490	—	.	nd
AtbZIP47	At5g65210	D	TGA1	YES	AtbZIP60	At1g42990	—	.	nd
AtbZIP34	At2g42380	E	.	nd					
AtbZIP61	At3g58120	E	.	nd					
AtbZIP23	At2g16770	F	.	nd					
AtbZIP24	At3g51960	F	.	nd					
AtbZIP19	At4g35040	F	.	nd					

[a]group
[b]not detected

D, G, H, and S in the bZIP family with DNA sequences containing the ACGT core was confirmed (Table 1). On the other hand, no binding of group C proteins was observed. It has been reported that group C proteins in the bZIP family have conserved phosphorylation sites,[8] and that a maize group C bZIP protein, Opaque2, is modified by phosphorylation.[15] Hence group C proteins may need some modification such as phosphorylation for binding.

Transcription is controlled by binding of TFs to the transcription regulatory region (TRR) in the 5′-upstream region of a gene. Thus, for better understanding of the gene expression network, it is important to analyze the binding of a TF to the TRR of a gene. Initiation of flowering is regulated by many genes. Among these, the *FLC* and *LFY* genes are known to be important negative and positive regulators respectively.[16,17] Next we used the upstream regions of the *FLC* (At5g10140) and *LFY* (At5g61850) genes as the target TRR sequences and searched for the TFs binding to these TRRs. For this purpose, biotinylated target TRR fragments containing the respective 5′-regulatory regions (300 bp, encompassing the −450 to −150 bp upstream region from the start codon of each gene) were generated by PCR using 5′-biotin-labeled primers, and randomly selected 192 TFs were synthesized by a cell-free protein synthesis system using [^{14}C]leucine. We divided the ^{14}C-labeled TFs into eight groups, each of which contained 24 different TFs. Each group of TFs was then mixed and incubated with one of the biotin-labeled target TRR fragments. After incubation, the target TRR fragments were pulled down using streptavidin-conjugated magnetic beads. The beads were washed 3 times and then subjected to SDS–PAGE analysis. In our search for the TFs binding to the *FLC* TRR fragment, specific binding of a 44 kDa protein to the fragment was observed in a TF group (data not shown). Among the 24 TFs that were mixed and used in the binding assay in the group, three TFs had predicted molecular masses of about 44 kDa. The binding activities of these three candidates to the *FLC* fragment were individually examined by competition assay. The candidate proteins were incubated with a biotinylated *FLC* fragment in the presence and the absence of a non-labeled competitor DNA fragment, and finally the At3g12720 product (MYB67) was found bind specifically to the TRR region of the *FLC* gene (Fig. 1C). Following the same assay protocol, a protein synthesized from clone At4g36730 (G-box binding factor 1, GBF1) was found to be a specific binding protein for the *LFY* TRR fragment (Fig. 1C). MYB67 and GBF1 belong to the MYB and bZIP families respectively. Typical binding sequences for MYB ((C/T)AAC(T/G)G) and bZIP (G-box: CACGTG) TFs do not exist in TRR fragments used in these experiments, but similar sequences, TAAATG (−314 to −319) and CACATT (−201 to −206), were found in the *FLC* and *LFY* TRR fragments respectively. Binding of GBF1 to CACATT in the *LFY* TRR fragment was confirmed by DNA foot-printing analysis (data not shown). Although further experiments are required to determine whether MYB67 and GBF1 do in fact bind to those sequences in *FLC* and *LFY* TRR respectively *in vivo*, these results suggest that our TF protein library may help in large-scale screening for isolation of TFs that bind to the TRR of target genes. Furthermore, the result that a bZIP TF, GBF1, binds to a sequence not identical to the A-, C-, or G-boxes suggests that the bZIP TFs for which we did not detect binding activity with the A-, C-, or G-boxes in this study might also recognize similar sequences to those elements.

For genome-wide biochemical analysis, large-scale synthesis of proteins has so far been a technological bottleneck. Methodologically, it is impossible to achieve genome-scale synthesis of proteins by conventional methods using living cells. In contrast, our cell-free protein synthesis system from wheat embryo is very suitable for the large-scale production of proteins. We created a protein library consisting of 647 Arabidopsis TFs using the cell-free system in this study. Using the TF library, we demonstrated DNA-binding assay of bZIP TFs and screening of TF binding to the TRR of *FLC* and *LFY*. These results indicate that the quality of the protein library is sufficient for large-scale biochemical characterization. The cell-free based protein library might become a promising tool in genome-wide biochemical analysis. Recently, we also succeeded in establishing a protein microarray system based on this cell-free protein synthesis system.[18] We hope that appropriate use of these methods will accelerate the progress of the genome-wide biochemical analysis of proteins.

Acknowledgments

This work was partially supported by the program of Special Coordination Funds for Promoting Science and Technology of the Ministry of Education, Culture, Sports, Science, and Technology of Japan (financial support to T.S. and Y.E.).

References

1) International Human Genome Sequencing Consortium, *Nature*, **409**, 860–921 (2001).
2) Riechmann JL, Heard J, Martin G, Reuber L, Jiang CZ, Keddie J, Adam L, Pineda O, Ratcliffe OJ, Samaha RR, Creelman R, Pilgrim M, Broun P, Zhang JZ, Ghandehari D, Sherman BK, and Yu GL, *Science*, **290**, 2105–2110 (2000).
3) Madin K, Sawasaki T, Ogasawara T, and Endo Y, *Proc. Natl. Acad. Sci. USA*, **97**, 559–564 (2000).
4) Sawasaki T, Ogasawara T, Morishita R, and Endo Y, *Proc. Natl. Acad. Sci. USA*, **99**, 14652–14657 (2002).
5) Seki M, Narusaka M, Kamiya A, Ishida J, Satou M, Sakurai T, Nakajima M, Enju A, Akiyama K, Oono Y, Muramatsu M, Hayashizaki Y, Kawai J, Carninci P, Itoh M, Ishii Y, Akazawa T, Shibata K, Shinagawa A, and Shinozaki K, *Science*, **296**, 141–145 (2002).
6) Sawasaki T, Morishita R, Gouda MD, and Endo Y, *Methods Mol. Biol.*, **375**, 95–106 (2007).
7) Sawasaki T, Hasegawa Y, Tsuchimochi M, Kamura N, Ogasawara T, Kuroita T, and Endo Y, *FEBS Lett.*, **514**, 102–105 (2002).
8) Jakoby M, Weisshaar B, Droge-Laser W, Vicente-Carbajosa J, Tiedemann J, Kroj T, and Parcy F, *Trends Plant Sci.*, **7**, 106–111 (2002).
9) Izawa T, Foster R, Nakajima M, Shimamoto K, and Chua NH, *Plant Cell*, **6**, 1277–1287 (1994).
10) Kobayashi T, Kodani Y, Nozawa A, Endo Y, and Sawasaki T, *FEBS Lett.*, **582**, 2737–2744 (2008).
11) Lara P, Oñate-Sánchez L, Abraham Z, Ferrándiz C, Díaz I, Carbonero P, and Vicente-Carbajosa J, *J. Biol. Chem.*, **278**, 21003–21011 (2003).
12) Satoh R, Fujita Y, Nakashima K, Shinozaki K, and Yamaguchi-Shinozaki K, *Plant Cell Physiol.*, **45**, 309–317 (2004).
13) Lee SS, Yang SH, Berberich T, Miyazaki A, and Kusano T, *Plant Biotechnol.*, **23**, 249–258 (2006).
14) Kaminaka H, Näke C, Epple P, Dittgen J, Schütze K, Chaban C, Holt III BF, Merkle T, Schäfer E, Harter K, and Dangl JL, *EMBO J.*, **25**, 4400–4411 (2006).
15) Ciceri P, Gianazza E, Lazzari B, Lippoli G, Genga A, Hoschek G, Schmidt RJ, and Viotti A, *Plant Cell*, **9**, 97–108 (1997).
16) Alexandre CA and Hennig L, *J. Exp. Bot.*, **59**, 1127–1135 (2008).
17) Sablowski R, *J. Exp. Bot.*, **58**, 899–907 (2007).
18) Sawasaki T, Kamura N, Matsunaga S, Saeki M, Tsuchimochi M, Morishita R, and Endo Y, *FEBS Lett.*, **582**, 221–228 (2008).

Journal of Experimental Botany, Vol. 60, No. 11, pp. 3067–3073, 2009
doi:10.1093/jxb/erp134 Advance Access publication 8 May, 2009
This paper is available online free of all access charges (see http://jxb.oxfordjournals.org/open_access.html for further details)

Journal of Experimental Botany
www.jxb.oxfordjournals.org

RESEARCH PAPER

Isolation and identification of ubiquitin-related proteins from *Arabidopsis* seedlings

Tomoko Igawa[1,*], Masayuki Fujiwara[1], Hirotaka Takahashi[2], Tatsuya Sawasaki[2], Yaeta Endo[2], Motoaki Seki[3], Kazuo Shinozaki[3], Yoichiro Fukao[1] and Yuki Yanagawa[1,*,†]

[1] The Plant Science Education Unit, The Graduate School of Biological Sciences, Nara Institute of Science and Technology, 8916-5 Takayama-cho, Ikoma, Nara 630-0101, Japan
[2] Cell-Free Science and Technology Research Center, Ehime University, 3 Bunkyo-cho, Matsuyama, Ehime 790-8577, Japan
[3] RIKEN Bioresource Center, 3-1-1 Takayama-cho, Tsukuba, Ibaraki 305-0074, Japan

Received 15 December 2008; Revised 9 March 2009; Accepted 6 April 2009

Abstract

The majority of proteins in eukaryotic cells are modified according to highly regulated mechanisms to fulfill specific functions and to achieve localization, stability, and transport. Protein ubiquitination is one of the major post-translational modifications occurring in eukaryotic cells. To obtain the proteomic dataset related to the ubiquitin (Ub)-dependent regulatory system in *Arabidopsis*, affinity purification with an anti-Ub antibody under native condition was performed. Using MS/MS analysis, 196 distinct proteins represented by 251 distinct genes were identified. The identified proteins were involved in metabolism (23.0%), stress response (21.4%), translation (16.8%), transport (6.7%), cell morphology (3.6%), and signal transduction (1.5%), in addition to proteolysis (16.8%) to which proteasome subunits (14.3%) is included. On the basis of potential ubiquitination-targeting signal motifs, in-gel mobilities, and previous reports, 78 of the identified proteins were classified as ubiquitinated proteins and the rest were speculated to be associated proteins of ubiquitinated proteins. The degradation of three proteins predicted to be ubiquitinated proteins was inhibited by a proteasome inhibitor, suggesting that the proteins were regulated by Ub/proteasome-dependent proteolysis.

Key words: *Arabidopsis* seedling, MS, ubiquitin-related protein.

Introduction

Ubiquitin (Ub)-mediated protein modification is a critical post-translational regulatory mechanism that occurs in all eukaryotic cells. The conserved 76 amino acid polypeptide, Ub, is covalently attached to a substrate protein as a signal molecule, and this attachment leads to various outcomes. The widely known fate of ubiquitinated proteins is degradation by 26S proteasome, one specific case being that more than four Ubs comprise a multi-Ub chain via lysine (K) 48 residues (Thrower *et al.*, 2000). Other types of ubiquitination, such as mono-ubiquitination and non-canonical ubiquitination, are implicated in various cellular functions, including endocytosis, endosomal sorting, signal transduction, and DNA damage repair (reviewed by Haglund and Dikic, 2005). Ubiquitination of target proteins requires the sequential action of three enzymes: Ub-activating enzyme (E1), Ub-conjugating enzyme (E2 or UBC), and Ub ligase (E3) (Hershko and Ciechanover, 1998; Pickart, 2001). The completely sequenced *Arabidopsis* genome has enabled the prediction of plant ubiquitination enzymes. To date, the activities of two E1s (Hatfield *et al.*, 1997) and 25 E2s (Kraft *et al.*, 2005) have been experimentally proven, and 12 genes encoding UBC domains are predicted to be E2s on the basis of their sequences (Bachmair *et al.*, 2001). Similar to other organisms, *Arabidopsis* E3s are predicted to form the largest

* These authors contributed equally to this work.
† To whom correspondence should be addressed: E-mail: yyana@bs.naist.jp
Abbreviations: DET3, de-etiolated 3; FBA, fructose biphosphate aldolase-like; GAPC, glyceraldehyde-3-phosphate dehydrogenase C subunit; ORF, open reading frame; Ub, ubiquitin; V-ATPase, vacuolar H^+-ATPase.

family comprising more than 1400 genes (Mazzucotelli *et al.*, 2006). Furthermore, the presence of additional proteins, such as an enhancer of E2, has been reported (Yanagawa *et al.*, 2004). Clearly, numerous proteins are involved in Ub-mediated protein regulation.

To identify ubiquitinated proteins in yeasts and mammals, several proteomic approaches that utilize various purification methods and MS/MS analyses have been reported (Peng *et al.*, 2003; Hatakeyama *et al.*, 2005; Jeon *et al.*, 2007). In plants, two groups recently reported the proteomics of ubiquitinated proteins from *Arabidopsis* cell cultures and seedlings, respectively (Maor *et al.*, 2007; Manzano *et al.*, 2008). Meanwhile, a Ub-related proteome that includes both ubiquitinated proteins and their associated proteins has been reported only in human cells (Matsumoto *et al.*, 2005).

As many proteins show spatiotemporal expression during development/life cycle, it is speculated that Ub-related proteins also vary among distinct tissues at various developmental stages. Therefore, the accumulation of information of Ub-related proteins from differentiated tissues at various stages would facilitate an understanding of Ub-mediated protein regulation throughout the life cycle. In addition, to make a comparison with the reports of Maor *et al.* (2007) and Manzano *et al.* (2008) that provided useful information of ubiquitinated proteomes from non-differentiated cell cultures and *Arabidopsis* seedlings, respectively, the proteomic analysis of Ub-related proteins expressed in *Arabidopsis* seedlings was performed in this study. For the large-scale isolation of Ub-related proteins, the purification was performed under native conditions. Previous studies of *Arabidopsis* ubiquitinated proteomes utilized different Ub-binding domains (UBAs) and showed that each UBA has distinct specificity for ubiquitinated proteins (Maor *et al.*, 2007; Manzano *et al.*, 2008). In order to overcome the limited specificity for target recognition, an anti-Ub antibody was applied to isolate Ub-related proteins. This study could provide helpful information for future work related to Ub-mediated protein regulation in plants.

Materials and methods

Plant materials

Arabidopsis (ecotype Columbia) seeds were germinated and cultured with shaking in liquid Murashige and Skoog medium containing 1% sucrose and 0.5 g l^{-1} MES, under a 16/8 h light/dark cycle at 22 °C. MG132 (Peptide Institute, Inc., Osaka, Japan) was added to 10-d-old cultured seedlings at a final concentration of 10 μM. After 24 h treatment, the seedlings were harvested. *Nicotiana benthamiana* was grown in a temperature-controlled growth room maintained at 25 °C under a 16/8 h light/dark cycle. Four- to five-week-old plants were used for experiments.

Large-scale purification of Ub-related proteins

To prepare an immunoaffinity column, HiTrap NHS-activated HP (1 ml, GE Healthcare Amersham Biosciences KK, Tokyo, Japan) was coupled with 1 mg of anti-Ub antibody FK2 (Nippon Bio-Test Laboratories, Tokyo, Japan) or mouse serum (Chemicon International, Inc., California, USA) as a negative control according to the manufacturer's instructions.

To purify Ub-related proteins under native condition, *Arabidopsis* seedlings were ground in liquid N_2 with a mortar and pestle, and the powder was further ground in buffer A [50 mM TRIS-HCl (pH 7.5), 150 mM NaCl] containing the Complete Protease Inhibitor cocktail (Roche Applied Science, GmbH, Mannheim, Germany), 5 mM 2-mercaptoethanol, and 10 μM MG132. The homogenate was centrifuged at 32 300 *g* for 15 min and the supernatant was centrifuged again for 5 min. The supernatant was filtered through a 0.8 μm syringe filter. The total protein extract (200–250 mg) was applied to an immunoaffinity column equilibrated with buffer A. After washing the column with 5 vols of buffer A, bound proteins were eluted with buffer B [0.1 M glycine-HCl (pH 3.0), 150 mM NaCl]. Purification of the Ub-related proteins was performed three times.

In-gel digestion of purified proteins, MS/MS analysis, and data reduction

The eluted proteins from three independent purifications were mixed and fractionated by SDS-PAGE. Protein bands were detected with Flamingo™ Fluorescent Gel Stain (Bio-Rad Laboratories, CA, USA). The protein bands were excised and other smearing regions were cut into 2-mm-long gel pieces for in-gel trypsin digestion. In-gel digestion and MS/MS analysis were performed according to the methods described by Fujiwara *et al.* (2006) and Nakashima *et al.* (2008). The gel pieces were dehydrated by washing twice with 100% acetonitrile, and dried with a vacuum concentrator. The proteins were reduced with 10 mM DTT at 56 °C for 45 min and then alkylated with 55 mM iodoacetamide at room temperature in the dark for 30 min. After washing twice with 25 mM ammonium bicarbonate, the samples were dehydrated again with 50% acetonitrile and dried. The protein samples were digested with 10 μg ml^{-1} proteomics-grade trypsin (Promega, Madison, WI, USA) for 12 h at 37 °C.

The digested peptides were subjected to column chromatography (PEPMAPC18, 5 μm, 75 μm internal diameter, 15 cm; Dionex, Sunnyvale, CA) using the CapLC system (Waters, Milford, MA, USA). Buffers were 0.1% formic acid in water (A) and 0.1% formic acid in acetonitrile (B). A linear gradient from 5% to 45% B for 25 min was applied, and peptides eluted from the column were introduced directly into a Q-TOF Ultima mass spectrometer (Waters) at a flow rate of 100 nl min^{-1}. In the ESI-positive ion mode, ionization was performed at a capillary voltage of 2.2 kV with the PicoTip nanospray source (New Objective, Cambridge, MA). For survey scan, mass spectra were acquired for the two most intense ions from the precursor ion scan between m/z 400 and 1500. For collision-induced dissociation (CID), the collision energy was set automatically according to the mass and charge state of the precursor peptide. MS/MS spectra were analysed with the MASCOT server against a protein database from the

National Center for Biotechnology Information. The applied MASCOT search parameters were as follows: (i) taxonomy: *Arabidopsis thaliana*; (ii) potential modifications: carbamidomethyl and oxidation as fixed modifications, myristoylation (N-term G, K); (iii) max missed cleavage: 1; (iv) peptide tolerance: ±0.5 Da; (v) MS/MS tolerance: ±0.2 Da; and (vi) peptide charge: 2^+ and 3^+. Proteins detected from peptide fragments with high reliability [MASCOT score >40 (P <0.05)] were selected as identified proteins.

The presence of putative motifs in the identified proteins was analysed using Eukaryotic Linear Motif resource (ELM; http://elm.eu.org/) for destruction-box (D-box) and KEN-box, and GENETYX-MAC software for PEST sequences.

Antibody production

To produce a polyclonal fructose biphosphate aldolase-like (FBA) antibody, the open reading frame (ORF) of *Arabidopsis* FBA (At3g52930) was amplified with primers 'fructose AntiB-F' (5′-GGAATTCCATATGTCTGCCTTCACAAGCAA-3′) and 'fructose AntiB-R' (5′-CGGAATTCTCAGTACTTGTAATCCTTCACG-3′), thereby introducing a *Nde*I site at the 5′ terminus and an *Eco*RI site at the 3′ terminus. The *Nde*I–*Eco*RI fragment of FBA was cloned into the expression vector pET28c (+) carrying 6×-histidine at the N terminus. The resulting plasmid was transformed into BL21 (DE3) cells. The purified histidine-tagged FBA protein was injected into a rabbit as the antigen. The antiserum obtained was used as anti-FBA antibody for immunoblot analysis.

Agroinfiltration

The ORFs of At1g12840 (de-etiolated 3; DET3) and At3g04120 (glyceraldehyde-3-phosphate dehydrogenase C subunit; GAPC) were amplified from RIKEN *Arabidopsis* Full-Length cDNAs (RAFL) using the following primers: 'attB1-At1g12840-5'' (5′-GGGGACAAGTTTGTACAAAAAAGCAGGCTTCATGACTTCGAGATAT-3′) and 'attB2-At1g12840-3'' (5′-GGGGACCACTTTGTACAAGAAAGCTGGGTCAGCAAGGTTGATAGT-3′), and 'attB1-At3g04120-5'' (5′-GGGGACAAGTTTGTACAAAAAAGCAGGCTTCATGGCTGACAAGAAG-3′) and 'attB2-At3g04120-3'' (5′-GGGGACCACTTTGTACAAGAAAGCTGGGTCGGCCTTTGACATGTG-3′), respectively. Transfer of the PCR products to the entry vector pDONR221 was performed by BP reaction (Gateway; Invitrogen). Each ORF fragment of At1g12840 and At3g04120 on pDONR221 was transferred to the binary vector pGWB14 (Nakagawa *et al.*, 2007) carrying 3× HA by LR reaction (Gateway; Invitrogen).

The resulting constructs (DET3-HA and GAPC -HA) were introduced into *Agrobacterium tumefaciens* strain GV3101 by electroporation. Agroinfiltration using *N. benthamiana* leaves was performed as described previously (Katou *et al.*, 2005). Discs were collected from leaves infiltrated with *Agrobacterium* cells after infiltration for 2 d.

Degradation assays

For the degradation assays of DET3-HA and GAPC-HA proteins, total protein was extracted from agro-infiltrated *N. benthamiana* leaf discs with extraction buffer C (50 mM TRIS-HCl, 2 mM ATP, 5 mM $MgCl_2$, 10 mM 2-mercaptoethanol, and 20% glycerol) supplemented with 30 μM MG132 or DMSO. For the FBA degradation assay, total protein from *Arabidopsis* seedlings was extracted with buffer C supplemented with 10 μM leupeptin (Peptide Institute) and 30 μM MG132 or DMSO. The protein extracts were incubated at room temperature for 2 h. 3× SDS sample buffer was added to stop the reaction, and the sample was used for immunoblot analysis. Anti-HA antibody was purchased from Abcam plc (Cambridge, UK). The degradation assay for each protein was replicated three times. Signal intensities of proteins detected on immunoblotted membranes were quantitated by digitizing with Image J software (http://rsbweb.nih.gov/ij/). Each quantitated value of HA or FBA signal was divided by the corresponding quantitated value of the control protein. The relative amounts of the remaining proteins (%) after incubation with MG132 or DMSO were calculated.

Results and discussion

Purification and identification of Ub-related proteins from Arabidopsis *seedlings*

To isolate Ub-related proteins by immunoaffinity chromatography, monoclonal antibody FK2 was applied, which selectively recognizes the Ub moiety but not free Ub (Fujimuro *et al.*, 1994). Approximately 250 mg of total protein was obtained from 50 g of *Arabidopsis* seedlings and applied to the immunoaffinity column under native condition (Fig. 1A). The staining pattern of eluted proteins subjected to SDS–PAGE was reproducible among the samples derived from three independent purification steps (see Supplementary Fig. S1 at *JXB* online). Compared to the mouse serum column, a number of discrete bands on a smeared background were detected in the purified sample eluted with the FK2 column (Fig. 1B), suggesting different mobilities in a gel caused by the heterogeneity of multi-Ub chains, as observed in a study of human cells (Matsumoto *et al.*, 2005).

Numerous Ubs were detected by MS/MS analysis, indicating that they were probably derived from Ub-conjugated proteins. Ubs and E2 proteins were eliminated from the list of proteins isolated with the FK2 column and the proteins isolated with the mouse serum column were further subtracted. In this study, only proteins with a score of over 40 (P <0.05) were selected as candidate proteins with high reliability. Accordingly, 196 proteins, which were represented by 251 distinct genes including possible paralogs, were determined as Ub-related proteins (see Supplementary Table S1 at *JXB* online). Comparing the

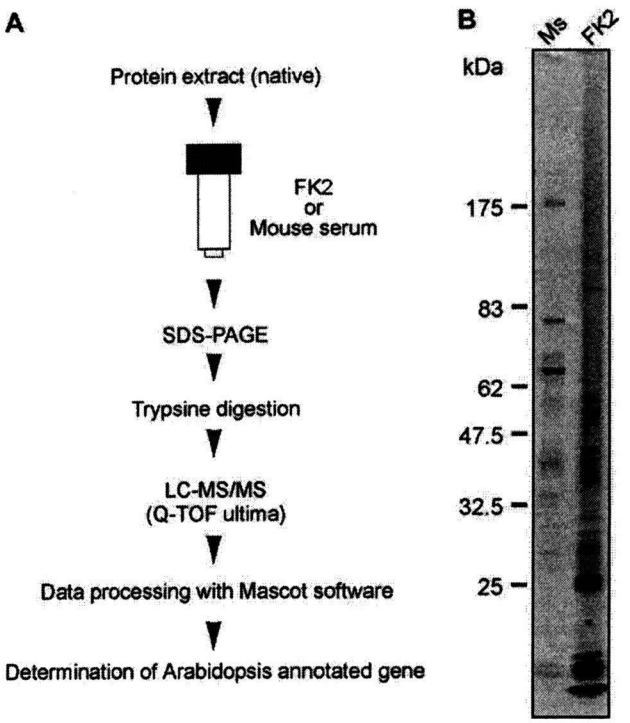

Fig. 1. Immunoaffinity purification and identification of Ub-related proteins. (A) Flow chart of purification and identification of Ub-related proteins. (B) Immunopurified proteins with FK2 or mouse serum (Ms) from *Arabidopsis* seedlings were subjected to SDS-PAGE and stained with Flamingo™.

results of this study with *Arabidopsis* ubiquitinated proteomes reported in two studies, 33 proteins were overlapped and only one protein (β-tubulin; protein no. 137 in Supplementary Table S1 at *JXB* online) was common to the three studies (see Supplementary Table S1 at *JXB* online). The low overlapping result compared to the previous studies may be due to the difference in the differentiation state of the protein source. In addition, unstructured threshold settings for protein screening from the MS scores may account for the difference in listed proteins among the three studies. The following reasons are proposed. Immunopurification with FK2 used in this study, enabled recognition of all types of ubiquitinated proteins, whereas each UBA used in the other studies had distinct specificity to ubiquitinated proteins. Therefore, the dominant ubiquitinated proteins were preferentially trapped by FK2. In addition, our dataset included a high proportion of associated proteins of ubiquitinated proteins due to the native condition used in protein purification. In fact, proteins annotated as RING-type E3 (protein no. 109 in Supplementary Table S1 at *JXB* online) and putative Ub receptors, DNA-repair protein RAD23 (protein no. 119 in Supplementary Table S1 at *JXB* online), and UBA-like motif-containing protein (protein no. 196 in Supplementary Table S1 at *JXB* online), were identified in this study, suggesting that non-direct target proteins for ubiquitination were also isolated.

Characterization of Ub-related proteins from Arabidopsis *seedlings*

The identified proteins were categorized on the basis of the biological processes described in 'The *Arabidopsis* Information Resource' (TAIR) (Fig. 2A). The large population of proteins involved in metabolism (23.0%) as well as previous *Arabidopsis* ubiquitinated proteomes (Maor *et al.*, 2007; Manzano *et al.*, 2008) may indicate the significance of ubiquitination for protein regulation in cellular metabolism. Similar to the previous report of Manzano *et al.* (2008), it was found that the proteins involved in stress response (21.4%) were more abundant in seedlings than in cell cultures. This might be due to the differentiation state of the cells, because the growth condition in liquid culture seemed to be more stressful for seedlings than for cell cultures. Indeed, proteins involved in abiotic stress were dominant in this category (Fig. 2A). The majority of translational proteins identified in our study (16.8%) were ribosomes, in agreement with Maor's study (Maor *et al.*, 2007). It has been speculated that ubiquitination might play an important role in the regulation and/or quality control of ribosomal proteins, as reported in human cells (Matsumoto *et al.*, 2005). In addition, the recent report by Kraft *et al.* (2008) of a link between ubiquitination and regulated degradation of mature ribosomes in yeast also supports our results. The percentage of proteins involved in signal transduction (1.5%) was lower than that previously reported for the ubiquitinated proteome from *Arabidopsis* seedlings (Manzano *et al.*, 2008). The difference may depend on the threshold for the screening of identified proteins from MS scores, as described above. Only proteins with a high reliability (95% confidence) were listed in this study, whereas Manzano's list contained proteins with low reliability (Manzano *et al.*, 2008). The proportions of other components were similar to that found in previous *Arabidopsis* ubiquitinated proteomes. One significant difference compared to the previous *Arabidopsis* ubiquitinated proteomes was the high percentage of proteasome subunits (14.3%), which was probably dependent on the native condition for protein purification. This fact indicated that the associated proteins of ubiquitinated proteins were isolated as well, and implied that most proteins were involved in Ub/proteasome-dependent proteolysis.

Classification of identified proteins

Purification under native condition is a feasible technique to identify Ub-related proteins that play major roles in Ub-dependent regulation (Matsumoto *et al.*, 2005). Since the protein population isolated under native condition included not only ubiquitinated proteins but also their associated proteins, they were classified as ubiquitinated proteins and their associated proteins based on the following three criteria.

First, previous *Arabidopsis* ubiquitinated proteomes from cell cultures and seedlings, respectively, were examined (Maor *et al.*, 2007; Manzano *et al.*, 2008). Of the proteins identified in our study, 33 have been reported as

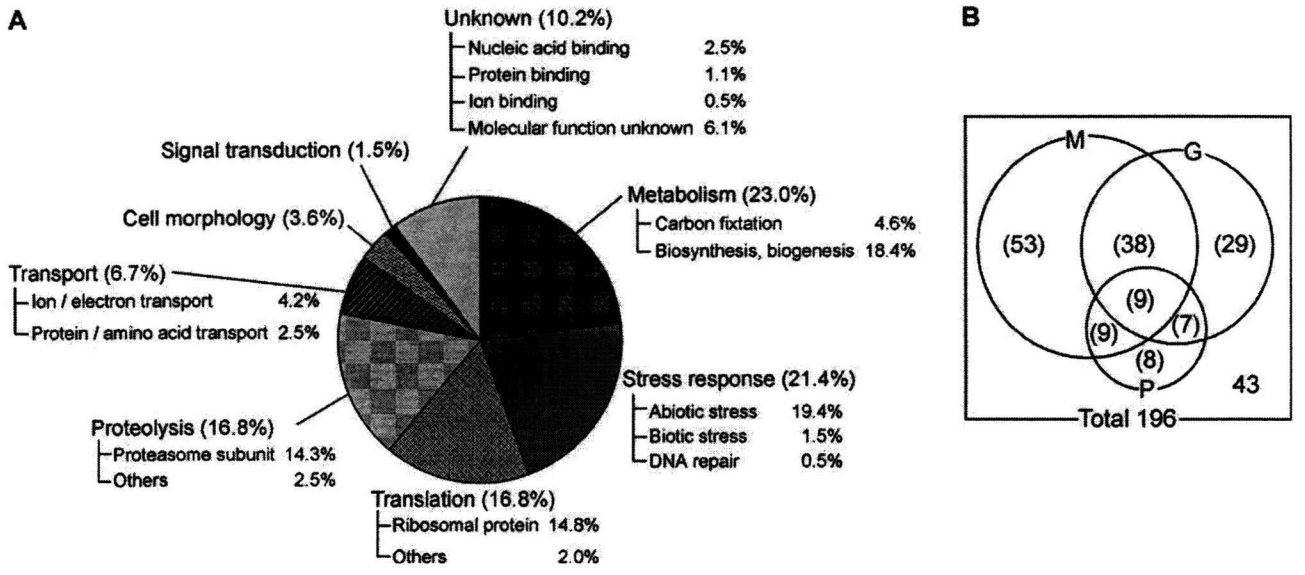

Fig. 2. Characterization of proteins identified from *Arabidopsis* seedlings. (A) Proportion of identified proteins categorized according to function. Each category was further subdivided according to specific function. (B) Numbers of potential ubiquitinated proteins and their associated proteins. Number outside the circles indicates the number of associated proteins of ubiquitinated proteins. M, proteins containing at least one motif; G, proteins detected in multiple gel pieces; P, proteins previously reported as ubiquitinated proteins.

ubiquitinated proteins, suggesting that these were the potential direct targets of ubiquitination (Fig. 2B; see Supplementary Table S1 at *JXB* online).

Second, the identified proteins were classified on the basis of potential ubiquitination-targeting signal motifs (D-box, KEN-box, and PEST sequence) to predict the ubiquitinated proteins. D-box and KEN-box are short sequence elements in the substrates of the anaphase-promoting complex/cyclosome (APC/C), which is a multisubunit RING-type E3 (King *et al.*, 1996; Pfleger and Kirschner, 2000), and indeed, RING-type E3 (protein no. 109 in Supplementary Table S1 at *JXB* online) was found in our study. PEST sequences that are rich in proline (P), glutamic acid (E), serine (S), and threonine (T) were found in a number of short-lived proteins controlled by proteolysis, mostly via ubiquitin-mediated degradation. Almost half of the identified proteins (109/196 proteins (55.6%)) contained at least one motif, implying that they are the potential targets of Ub/proteasome-dependent proteolysis (Fig. 2B; see Supplementary Tables S1 and S2 at *JXB* online).

Third, multiple detections from different gel pieces implied multi-ubiquitination of the proteins, since the heterogeneity of multi-Ub chains accounted for the different mobilities in a gel. Of the identified 196 Ub-related proteins, 83 (42.3%) were found in 2–17 gel pieces of different sizes (Fig. 2B; see Supplementary Table S1 at *JXB* online), suggesting that the proteins were probably tagged with heterogeneous multi-Ub chains.

Considering potential ubiquitination-targeting signal motifs, in-gel mobilities of the identified proteins, and previous reports, 153 proteins (78.0%) were predicted as the potential targets of ubiquitination, including 109 potential target proteins (55.6%) of Ub/proteasome-dependent proteolysis, whereas the remaining proteins (21.9%) were potential molecules associated with the ubiquitinated proteins.

Degradation assays of proteins predicted as ubiquitinated proteins

The results suggested that a large proportion of the identified proteins were involved in Ub/proteasome-dependent proteolysis. Therefore, the identified proteins were examined by proteasome degradation assay. According to the prediction described above, three proteins predicted as potential ubiquitinated proteins, At1g12840 (DET3, protein no. 82 in Supplementary Table S1 at *JXB* online), At3g04120 (GAPC, protein no. 1 in Supplementary Table S1 at *JXB* online), and At3g52930 (fructose biphosphate aldolase-like; FBA, protein no. 6 in Supplementary Table S1 at *JXB* online), were chosen for the assay.

DET3 encodes subunit C of vacuolar H^+-ATPase (V-ATPase). V-ATPase is one of the major proton pumps that act to acidify intracellular compartments (Sze *et al.*, 2002) and DET3 is significantly responsible for its activity (Schumacher *et al.*, 1999). Since DET3 contains four D-box motifs and was detected in two gel pieces (Supplementary Table S1 at *JXB* online), regulation of DET3 protein by Ub/proteasome-dependent proteolysis was highly expected. DET3 protein tagged with 3× HA was transiently expressed in *N. benthamiana* leaves by agroinfiltration. The protein extract was incubated with MG132, a 26S proteasome inhibitor. As a result, it was found that DET3 protein degradation was inhibited by MG132 treatment but not DMSO treatment (Fig. 3A), indicating that it was conjugated with canonical Ub chains and then underwent the